MUSA
ON THE INTERACTION BETWEEN MUD AND SAND

Results of MUSA field measurement campaigns at Holwerd, the Netherlands

January, 2023; Results of MUSA field measurement campaigns at Holwerd, the Netherlands

TKI MUSA project

Author(s)

Márcio Boechat Albernaz, MSc

Leo C. van Rijn, Em. Prof

Doke C. Schoonhoven, MSc

Luitze M. Perk, MSc

Measurement plan

TKI MUSA project

Client	MUSA consortium
Contact	Luitze Perk
Reference	
Keywords	Sand, mud, laboratory experiments, field measurements

Document control	
Version	Final
Date	09-01-2023
Project nr.	11204950
Document ID	
Pages	63
Status	Final

Doc. version	Author	Reviewer	Approver	Publish
Concept1	Márcio Boechat Albernaz, MSc Leo C. van Rijn, Em Prof Doke C. Schoonhoven, MSc Luitze M. Perk, MSc	Thijs van Kessel		
Final	Márcio Boechat Albernaz, MSc Leo C. van Rijn, Em Prof Doke C. Schoonhoven, MSc Luitze M. Perk, MSc	Thijs van Kessel		

About the MUSA project

Estuaries and tidal basins form the transition zones between land and sea. They contain important habitats for flora and fauna and are extensively used by people, like for navigation. For ecological and navigational purposes, it is important to understand and predict the evolution of channels and shoals, including sedimentation rates and the composition of the bed sediments. The bed material of large estuaries and tidal basins largely consists of mixtures of mud and sand, with predominantly sandy channels and mainly muddy intertidal areas. The interaction between sand and mud, in combination with currents and waves, leads to complex dynamics in these areas, with migrating channels and shoals.

Much is known about the behaviour of the individual sediment fractions, but the knowledge and understanding of sand-mud interaction remains limited, as do the available tools and models to accurately predict the bed evolution and sediment transport rates in sand-mud areas. Existing models, like the ones by Van Ledden (2003), Soulsby & Clarke (2005) or Van Rijn (2007) have only limitedly been verified with observations due to a lack of good quality observational data. Also, none of the available approaches cover the complete spectrum of sand-mud interaction, which includes settling, erosion processes induced by the combination of waves and currents, and the bed shear stress. Therefore, in practice sand and mud fractions are often treated separately. This decoupled approach limits the predictive capacity of numerical models, and therefore the impact of human intervention such as deepening of channels and port construction on maintenance dredging volumes and other morphological changes.

In the MUSA-research project, a consortium of contractors, consultants and research organizations join forces to increase the understanding of sand-mud dynamics by means of fieldwork campaigns and laboratory experiments, and to implement this knowledge in engineering tools and advanced models for the prediction of mud and sand transport and associated morphology in tidal conditions with both currents and waves.

Summary

The overall goal of MUSA is to improve the engineering tools predicting the amount of erosion and deposition of mud-sand mixtures. The investigation and prediction of the erosion and deposition is based on both physical experiments and field data. Herein we present the results from the field measurement campaign executed at the Dutch Wadden Sea between the Holwerd Pier and Ameland Island during spring 2022.

The measurements were executed at 4 different places, one day per location, covering a wide variety of mud-sand bed percentages. Each day covered approximately a tidal cycle, especially the peak ebb and flood velocities, at one fixed location. The data acquisition focused on the near-bed flow velocities and sediment concentrations of both sand and mud. A tailor-made frame from WaterProof was deployed to collect detailed near-bed water-sediment samples and data about flow velocities, turbidity and sediment characteristics.

The four sites along the Holwerd channel covered sand percentages between 10 and 54%. The Ameland end of the channel is composed of sandy beds while the mud percentages are increasing towards the mud-dominated Holwerd Pier. The campaigns measured flow velocities up to 1.0-1.6 m/s and associated sediment concentrations of 1- 10 kg/m^3 up to values above 20 kg/m^3 associated with the passage of boats in the narrow channel. The sediment concentrations are generally higher near the peak ebb flow condition. During slack tides, the sediment concentrations decrease towards 0.1-1 kg/m^3. The sand concentrations respond in quasi-equilibrium conditions with the higher flow velocity while the mud concentrations are also controlled by advection.

The sediment transport equations of Van Rijn (2007) showed good agreement with the measured data in terms of sand concentrations. The best results were found when including the effect of mud in the critical shear stress of sand. However at higher flow velocities, i.e. > 1 m/s, the computed values are overestimated.

Contents

1 Introduction

The field measurements performed in the MUSA project aim to complement the laboratory experiments to explore the erosion and transport of mud-sand sediments under waves and currents in natural systems.

The goal of the field measurements is to acquire sediment concentrations and sediment composition over distinct hydrodynamic conditions and bed compositions and to compare the results with the laboratory flume experiments and theoretical formulations. The integrated analyses across these methods (i.e. laboratory, field and theory) will be used in the upcoming phases of MUSA to improve the prediction methods of erosion and sediment transport.

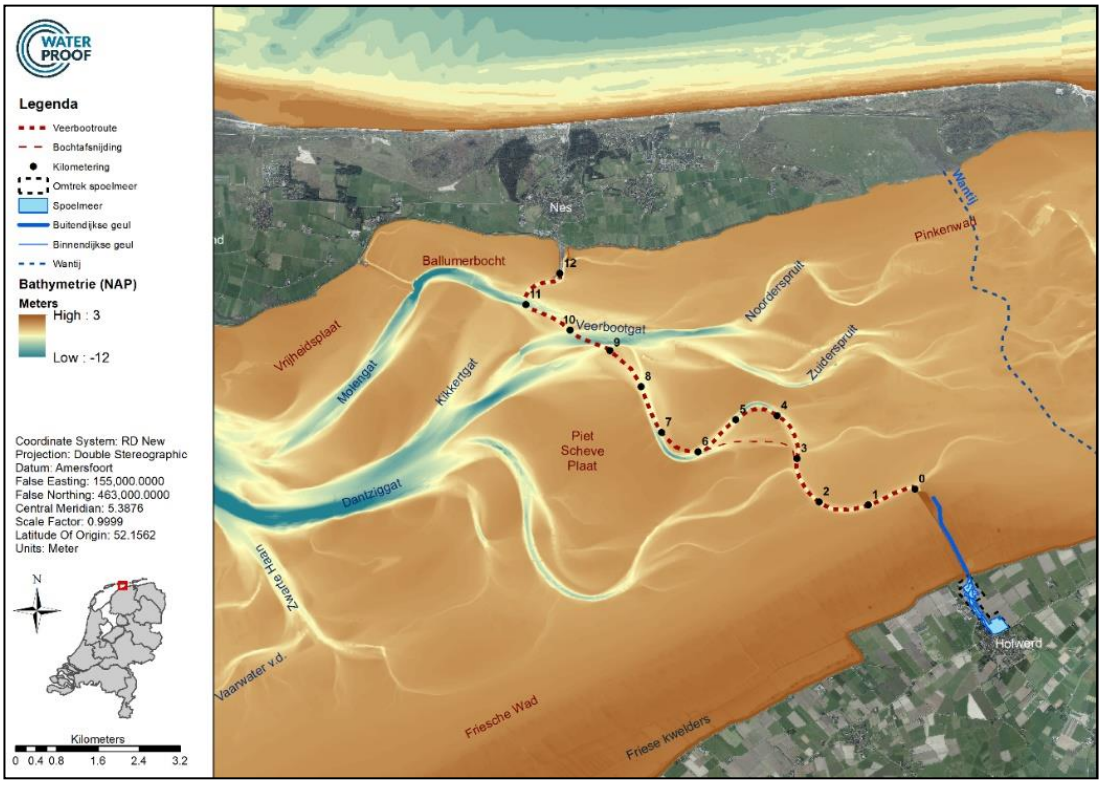

Figure 1 Overview of Wadden Sea between Ameland and Holwerd. The numbers correspond to Kilometric Points with respect to the Holwerd Pier.

The field measurements took place in the Dutch Wadden Sea between Holwerd and the Ameland Island (Figure 1). The Holwerd site has been selected due to its proximity, easy to access and the fact that the site is well known and described in the literature which will contribute to further analyses and comparisons.

The ferry channel from Holwerd to Ameland is located in the south-eastern part of the Borndiep tidal basin within the Wadden Sea. The tide is diurnal with a tidal range of approximately 1.6 m during neap tide and 3 m during spring tide. Wind-generated waves in the range of 0.3 to 1 m are generated in conditions with wind in the sector south-west to north-west. The flow volume through the channel is of the order 13 million m^3 per tide of approx. 6 hours. The maximum flow rate in the channel near Holwerd (over a distance of 4 to 5 km) varies between 200 and 300 m^3/s and the maximum flood current velocity is in the range of 1 to 1.5 m/s.

Four locations were chosen along the main channel between the Holwerd and Ameland ferry piers. The ferry channel shows a transition from sandy beds near the Ameland island towards muddy sediments near Holwerd. The ferry channel, especially near Holwerd, is intensively dredged (1 to 2 million m^3/year; 80% mud/silt and 20% sand) to keep a minimum sailing depth of 4 m. During flood tide, the dredged spoil is brough to a dumping site far away (at 10 km from Holwerd). During ebb tide, the dredged spoil is

discharged in the main channel at about 4 to 5 km from Holwerd; part of these sediments may flow back during the flood tide.

The field measurements were performed on 2 days in May (16, 17 May 2022) and 2 days in June (14, 15 June 2022) at 4 locations (Figure 2) closer to the Holwerd pier where there is a gradation from mud-rich sediments to sandier sediments towards the Ameland Island.

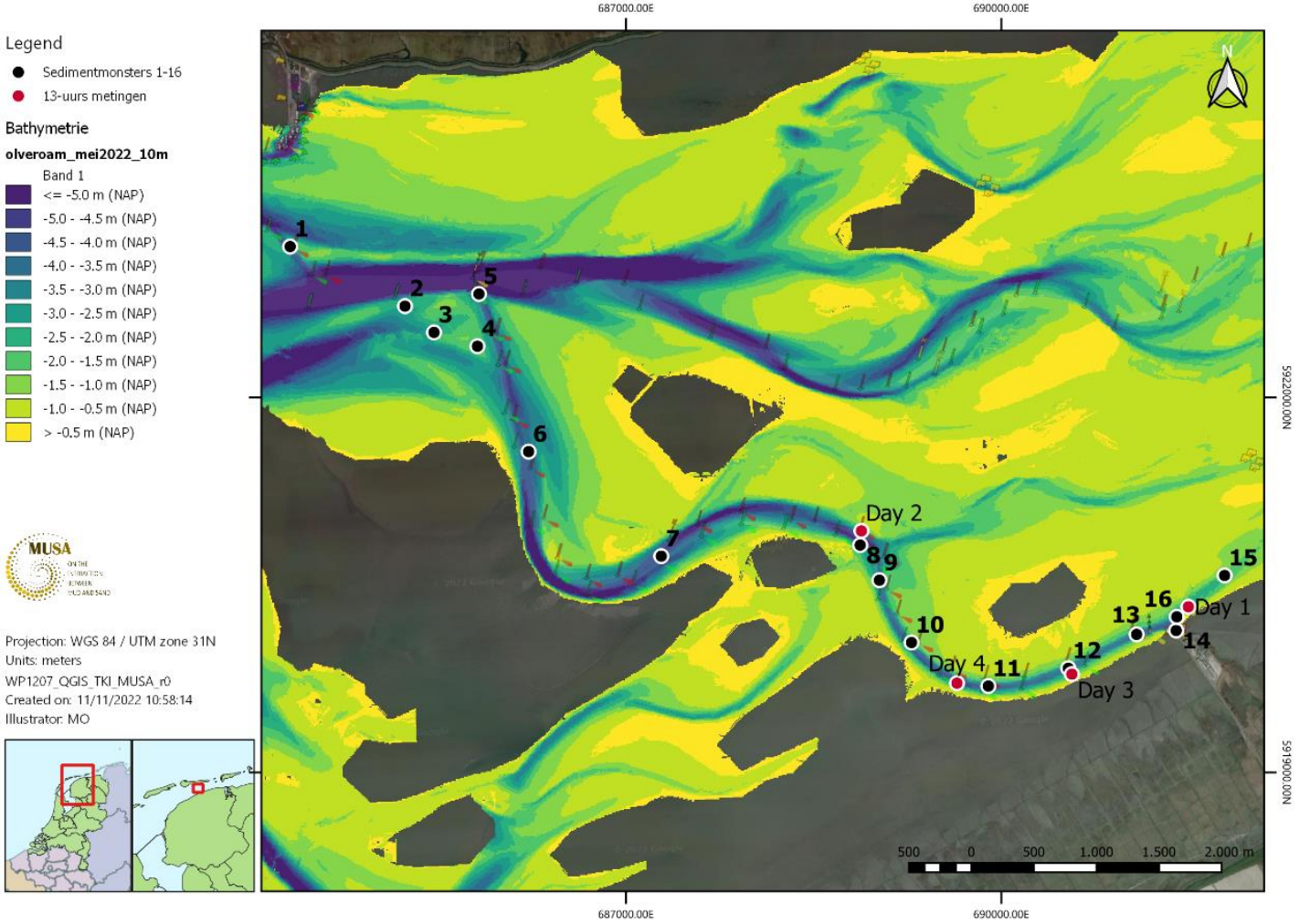

Figure 2 Measurement locations along the Holwerd-Ameland channel

2 Measurement campaign and instrumentation

The measurements were performed with the survey boat Bumblebee, (Figure 3) of WaterProof. The sediment transport measurements were done by deploying a tailor-made frame (Figure 4) of WaterProof for this campaign. The frame was designed to be self-standing on the bed and to self-align itself with the income flow while acquiring water-sediment samples and instrumental data. Bed samples from each location were taken by a Van Veen grab (VVG).

Each measurement day enclosed approximately a 10-hour period covering the maximum ebb and flood velocities which are most interesting for sediment transport.

Hydro-meteorological data are continuously measured in the vicinity of the measurement locations by Rijkswaterstaat (see <https://waterinfo.rws.nl>). The hydro-meteorological data are important to provide the background conditions, including tides, waves and wind, during the measurements.

2.1 Instrumentation

Water-sediment samples and instrumental data were collected on board of the Bumblebee at approximately 30 minutes intervals over 10 hours. The data enclosed flow velocity profiles near the bed, salinity, temperature, pressure, turbidity, sediment grain size and sediment concentrations with the following instruments:

- Aquadopp (Nortek) point velocity; measurement level at 1.1 - 1.2 m above the bed level;
- ADCP (Nortek Signature 1000 KHz) for near-bed profiles of velocities and sand concentrations (using dedicated echo-backscatter) in the near-bed layer of 1 m above the bed level (looking down ADCP mounted at about 1.2 m above the bed);
- CTD RBR Concerto for measuring conductivity, water temperature and pressure;
- OBS for suspended sediments (up to 5.000 mg/l); at 1 m above the bed on Day 1,2; at 0.7 m above the bed on Day 3,4;
- ValePort Altimeter for vertical reference (distance to water level and distance to seabed);
- LISST 100X Sequoia laser scatter to measure suspended sediment grain sizes (kindly borrowed from TUDelft)
- Water-sediment samples from Peristaltic pump (8 nozzles) over vertical height.

Figure 3 Photo of the Bumblebee boat from WaterProof at Holwerd.

The measurement frame (Figure 4) hosts 8 vertical positions for constant water-sediment intake and a face-down ADCP that samples the lowest meter of the water column just in front of the intake water tuber. The frame was designed to be placed over the seabed in order to acquire hydrodynamic and sediment data near the bed while being stable up to ca 1 m/s flow conditions at the same time as minimizing flow disturbances.

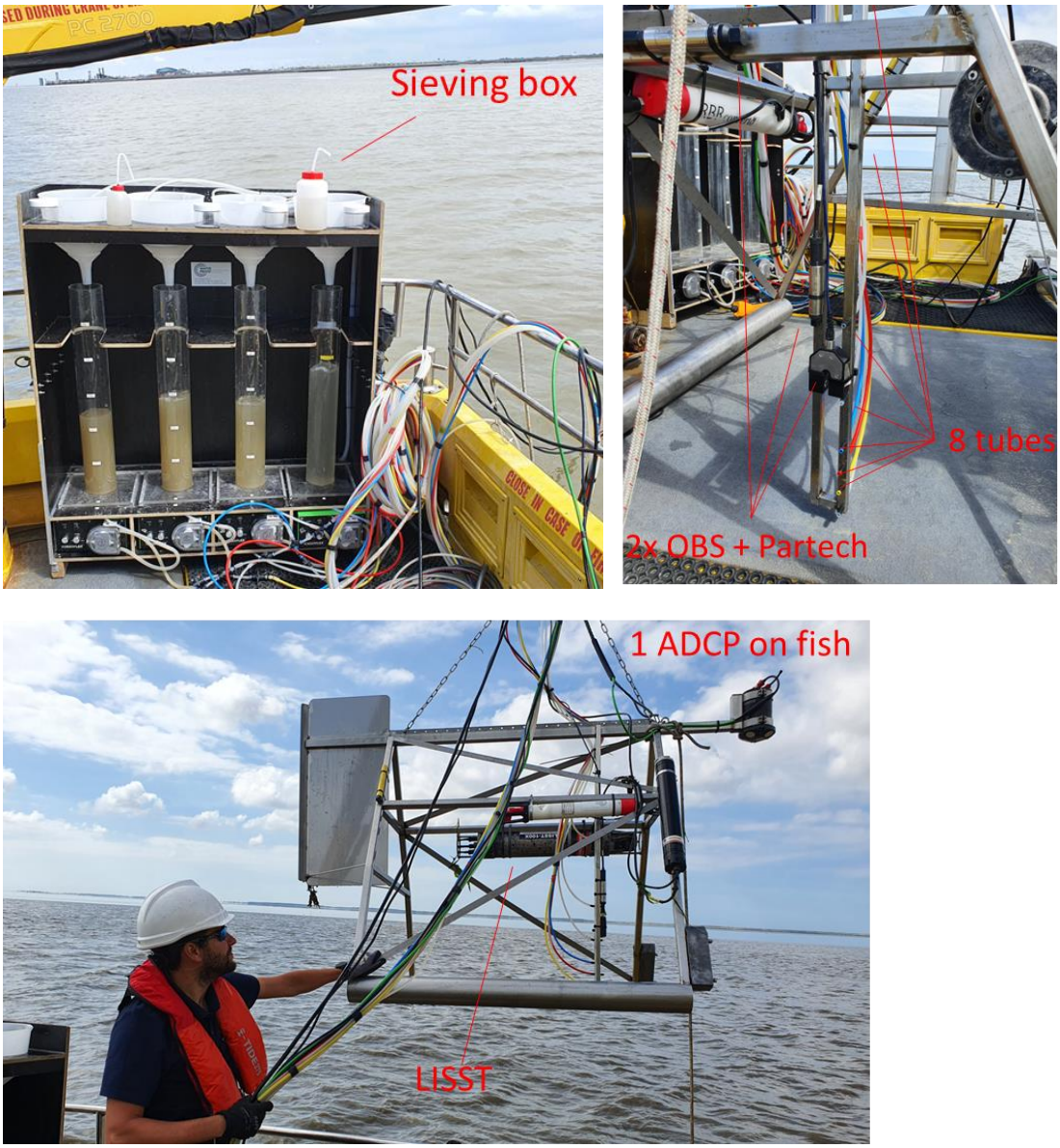

Figure 4 Setup of the measurement frame and water filtering.

The key instruments for sediment and hydrodynamic measurements were positioned (center of measuring volume) in the frame, as follows:

Pump heights from bottom (cm)	
A	5
B	10
C	15
D	25
E	40
F	70
G	100

ADCP height = 1.2 m (looking downwards with 10cm blank distance)

OBS (height G for Day 1, 2 and height F for Day 3, 4)

Aquadopp vel =~ 1.2 m above the bed

CTD RBR = 0.84 m from the bed

LISST = 0.75 m from the bed

[Mud] = Mud concentration from water samples

Water-sediment samples were pumped every 30 minutes, approximately, from the 8 different heights into 5 liters sampling tubes using the peristaltic pumps. During pumping the sand and mud contented were sorted by sieving the intake water with a 63 µm mesh. The fine mud material and suspended solid content was further filtered onboard with a 0.45 µm Millipore filter under vacuum pumps. Weighing and further processing of the samples was done in the WaterProof sediment laboratory.

Simultaneously to the water sampling, we continuously collected instrumental data about flow velocities, turbidity, salinity, pressure and suspended grain size. In order to assess the advected versus local suspended sediments, seabed samples were taken at each measuring site with a Van Veen Grab sampler (VVG).

The passage of ferries and other ships were registered due their effect on resuspending sediments within the narrow and shallow navigation channel.

2.2 Measurement program and procedure

The measurement program on each day consisted of:

1 travelling to the measurement location and positioning of the survey vessel by two anchors and a water-anchor;
2 sampling of bed material (Van Veen Grab);
3 deployment of bed frame with instrumentation;
4 start of pump operation for water-sediment samples (4 pumps over 5 minutes connected to 4 lowest pump intake nozzles); 5 liter samples are collected in a container with a 63-µm sieve on top of it to separate the sand fraction; the remaining mud sample was filtered with the Milipore filters and individually stored for further processing in the laboratory of WaterProof;
5 sand fraction is stored in pots for further processing in the laboratory of WaterProof;
6 same procedure for the 4 highest pump intake nozzles; time period between two pump rounds was 5 to 15 minutes;
7 measurement procedure is repeated every 30 minutes over the tidal cycle.

3 Results and analyses of the field measurements

Here we present the main results and preliminary analyses of the 4 days campaign in May and June 2022 in the Wadden Sea near Holwerd.

The results and analysis in this report intent to describe and explore the measured hydrodynamic and sediment transport data at Holwerd. We also performed preliminary analyses and comparison with sediment transport theories (e.g van Rijn 2007, 2015) and previous measurements (Deltares, 2016a,b, 2021; WaterProof 2021; Van Rijn, 2021), which are shown in Appendix B. The hydro-meteorological conditions are described in Section 3.1. The seabed composition and the measured sediment concentrations over the tidal cycle are described and analyzed in Sections 3.2 and 3.3, respectively.

3.1 Hydro-meteorological conditions

The most important characteristics of the tidal water levels and tidal currents are summarized in Table 3.1.

Based on the measured data, it follows

- the tides have tidal range values between 2.6 and 2.8 m on the measurement days and are close to maximum spring tide;
- the peak tidal current velocities are in the range of 0.75 to 1 m/s, except on the location Day 2 with peak values up to 1.5 m/s.
- wind was mild (<Bft 4) and thus wave activity was fairly low (wave height < 0.3 m) on all days (Day 1 to 4);
- the ebb peak current occurs about 1 hour after LW, while the flood peak flow occurs about 1 hour before HW; the time period between the ebb peak current and the flood peak current is relatively short with of 3 to 4 hours. That means a very short (or absent) low water slack period with a quick inversion from ebb to flood.

Table 3.1 Hydrodynamic and metocean conditions during the 4 days measurements

Date	Wind (Bft) waves (m)	Depth to NAP (m)	Tidal range (m)	Low Water to NAP (m)	High Water to NAP (m)	Ebb duration (hours)	Flood duration (hours)	Maximum ebb velocity (m/s)	Maximum flood velocity (m/s)
Day 1	Bft 4 <0.3	3.25	2.8	-1.2 16.00 hrs	1.6 21.30 hrs	5.6	6.2	0.75 17.00 hrs	0.75 20.30 hrs
Day 2	Bft 4 <0.3	3.0	2.8	-1.1 16.45 hrs	1.7 22.00 hrs	5.9	6.3	1.5 17.30 hrs	1.4 20.30 hrs
Day 3	Bft 3 <0.2	2.25	2.6	-1.1 15.30 hrs	1.5 21.5 hrs	5.7	6.3	0.8 16.30 hrs	0.9 20.00 hrs
Day 4	Bft 3 <0.2 m	3.7	2.6	-1.0 16.30 hrs	1.6 22.15 hrs	5.8	6.3	1.0 17.30 hrs	1.0 20.45 hrs

3.2 Seabed composition

Bed material were collected with a Van Veen Grab (VVG) along the Holwerd channel on 25 May 2022. The samples were taken in the direction from the Island of Ameland to Holwerd. In total 16 bed material samples were taken. The sampling locations are shown in Figure 5.

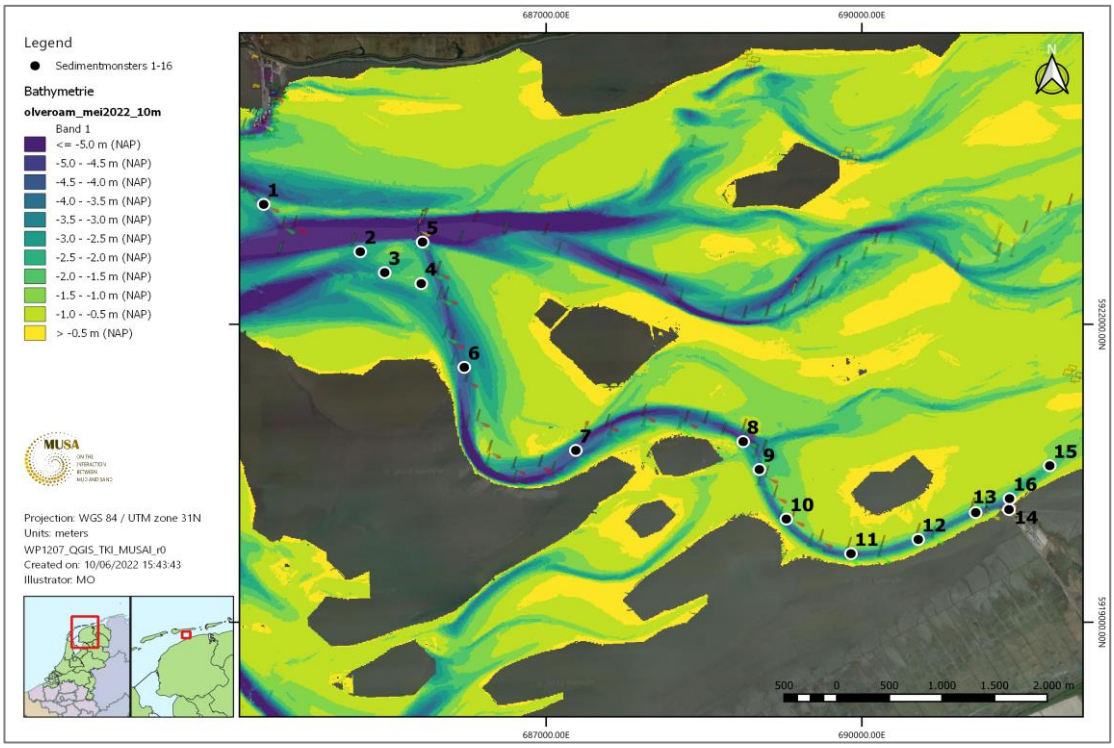

Figure 5 Locations of Van Veen bed samples from 25 May 2022

The bed samples (Figure 6) were characterized in terms of the percentage of sand and fines (mud) < 63 μm and the wet/dry bulk density. The results are presented in Table 3.2.

Figure 7 shows the percentage of fines and the dry bulk density along the channel. The new sediment samples are similar to the previous measurements. The channel near Holwerd (KPs -1 to 1) shows a large variation in terms of mud-sand composition, however, the first kilometers are generally mud-dominated. The basic trend of the bed material composition along the channel is a shift from muddy/silty bed materials near Holwerd (landward side) to more sandy bed materials towards the island of Ameland (seaward side). The percentage of fines is around 60% (±30%) close to the Holwerd pier which decreases to less than 10% at about 5 to 6 km and to below 3% close to Ameland. Locally, muddy spots can be found in sandy areas. For example, a very muddy sample was found at location 8 on May 2022 (Table 3.2), which is in the dumping area of dredged spoils during ebb tide.

The dry bulk density is around 800 (±300) kg/m³ close to Holwerd pier which increases to around 1400 (±300) kg/m³ further away.

Figure 8 shows the median particle size of the bed materials along the channel based on earlier data. The median grain size (d_{50}) of the sand fraction is around 110 (±30) μm close to Holwerd pier which increases to about 150 (±30) μm further away.

Following the approximation of dry bulk density based on the distribution of sand, mud and organics presented in the Phase 1AB report of MUSA, the empirical equation of Van Rijn and Barth (2019) is compared with the measured dry bulk density from the newly collected samples. The empirical equation relates the dry bulk density to the percentages of organic matter (p_{org}), clay (p_{clay}), silt (p_{silt})and sand (p_{sand}), as follows:

$$\rho_{dry} = (1-p_{org}/100)\,[400\,p_{clay}/100 + 800\,p_{silt}/100 + 1600\,p_{sand}/100] \qquad \text{equation 1}$$

with: $p_{clay}+p_{silt}+p_{sand}=100\%$.

Van Rijn and Barth (2019) is most valid for the top layer of natural mud-sand beds (e.g. 0.1 to 1 m) with p_{clay}/p_{silt} in the range of 20 to 30% at the end of the primary consolidation phase. The primary consolidation phase of a soft mud-sand layer with a thickness of about 1 m is of the order of 1 to 2 months depending on the percentage of sand. For a low sand content of 20% to 30%, the top layer can consolidate to 400–450 kg/m³ after about 1 month; and to about 600-700 kg/m³ after 1 month for a sand content of 30% to 50% (Van Rijn and Barth, 2019). Generally, the dry bulk density of the freshly deposited top layer (0.01 to 0.1 m) of the bed surface is smaller, e.g. up to 30% (see Table 3-4 of MUSA-Report 1A/1B). The thin upper part of the sediment layer in direct contact with the water column may have a much lower (fluffy) density of the order of 50% of the overall density of the top layer. Therefore, we expect variations when comparing the estimation from Equation 1 with measured dry bulk densities.

Table 3.3 and Figure 9 show the comparison of measured and predicted dry bulk density values. For the sediment dry density estimations, we considered the following assumptions: the percentage of fines < 63 μm is assumed to consist of clay <8 μm and silt particles 8-63 μm with a ratio of $p_{clay}/p_{silt}\cong 1/3$; the percentage organic materials are estimated to vary between 0% for very sandy samples to 5% for very muddy samples based on the visual inspection of the samples and early data from Holwerd; the dry bulk density of clay, silt and sand equals 400, 800 and 1600 kg/m³, respectively.

The predicted density values using commonly applied bulk densities for clay, silt and sand are on average 10% to 15% higher than the measured values. The systematic mismatch can be attributed to the aforementioned assumptions in the equation from Van Rijn and Barth (2019). For example, the equation assumes bulk densities for the different sediment fractions despite the fact that the predictor neglects the effect of consolidation and porosity which are important controls on the bulk density of cohesive (muddy) deposits.

Table 3.2 Bed material characteristics along the Holwerd ferry channel

Sample	Water depth (m)		Color	Wet/dry density (kg/m³)	% sand	Type of sediment
	Local	NAP				
1; KP10.4	4	4	dark grey	1758/1278	95	firm sand; no shell (≅200 μm)
2; KP9.2	2.5 (outside channel)	2.6	dark grey	1800/1467	98	firm sand; no shell (≅200 μm)
3; KP9.0	2.3 (outside channel)	2.4	dark grey	1867/1464	96	firm sand; no shell (≅200 μm)
4; KP8.5	1.5 (outside channel)	1.7	dark grey	1868/1442	97	firm sand; some shell (≅200 μm)
5; KP9	4	4.2	dark grey	1888/1483	99	firm sand; no shell (≅200 μm)

6; KP7.5	4	4.2	dark grey	1798/1391	97	firm sand; no shell (≅200 μm)
7; KP5.8	4	4.3		1964/1538	98	firm sand; no shell (≅200 μm)
8; KP3.3	4.4 (≅ 3.5 km from pier)	4.6	very dark grey	1440/732	17	slightly firm sandy mud; some shell
9; KP2.8	3.5	4.0	dark grey	1660/1084	73	soft sandy mud; some shell
10; KP2.4	3.6	4.0	dark grey	1649/1070	72	soft sandy mud with traces of very soft yellow-brown mud on top; some shell (Figure 3.3.2)
11; KP1.5	3.9	4.3	dark grey	1705/1114	78	soft sandy mud with traces of very soft yellow-brown mud on top; some shell
12; KP0.9	3.6	4.2	dark grey	1728/1167	77	soft sandy mud with traces of very soft yellow-brown mud on top
13; KP0.3	3.6	4.1	dark grey	1633/1236	64	soft sandy mud with traces of very soft yellow-brown mud on top; some shell
14; KP0	4 (in front of ferry pier)	4.5	dark grey	1629/992	49	soft sandy mud with traces of very soft yellow-brown mud on top; some shell
15;KP-0.6	1.5 (about 300 m beyond pier)	2.1	dark grey	1734/1159	73	soft sandy mud with traces of very soft yellow-brown mud on top; mussels and shells
16;KP-0.1	1.5 (at end of small pier)	2.2	dark yellow	1364/577	24	very soft yellow-brown mud (Figure 3.3.2)

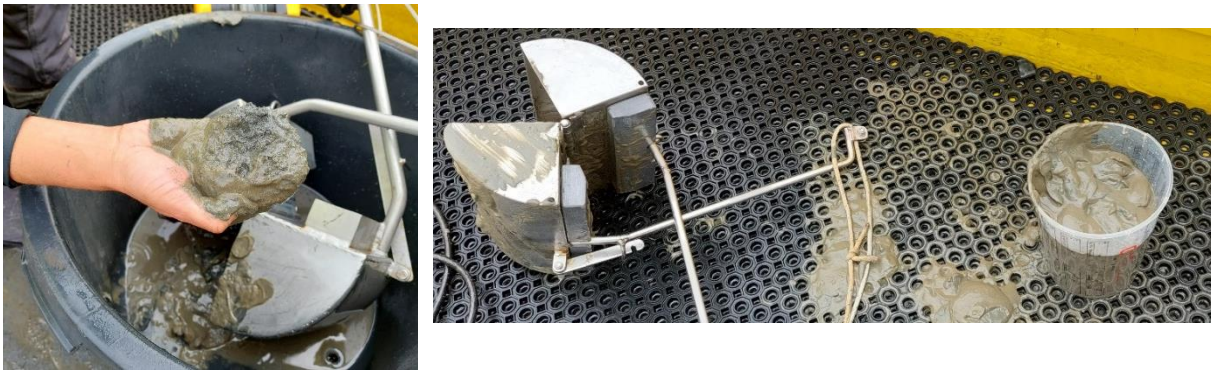

Figure 6 Sediments during sampling. Left: Soft sandy mud with dark yellow-brown traces of very soft mud on top; location 10. Right: Mud sample at location 16.

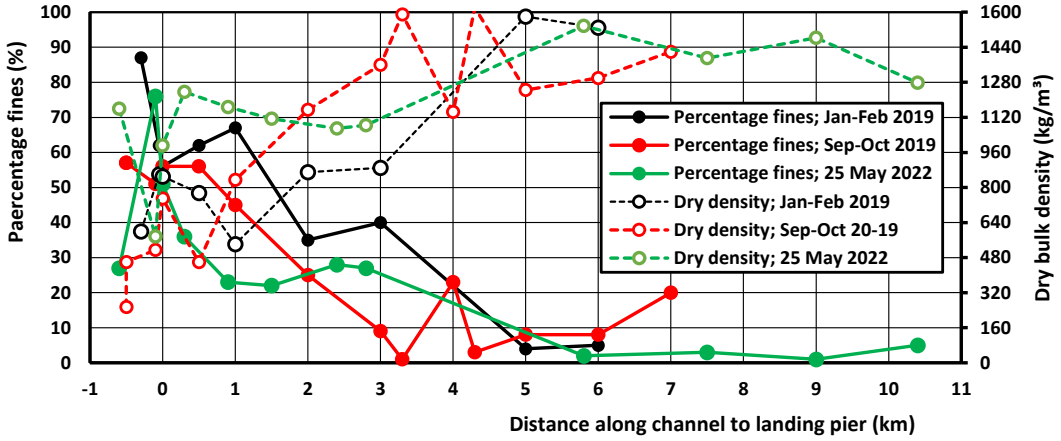

Figure 7 Percentage of fines < 63 μm and dry bulk density; Holwerd ferry channel.

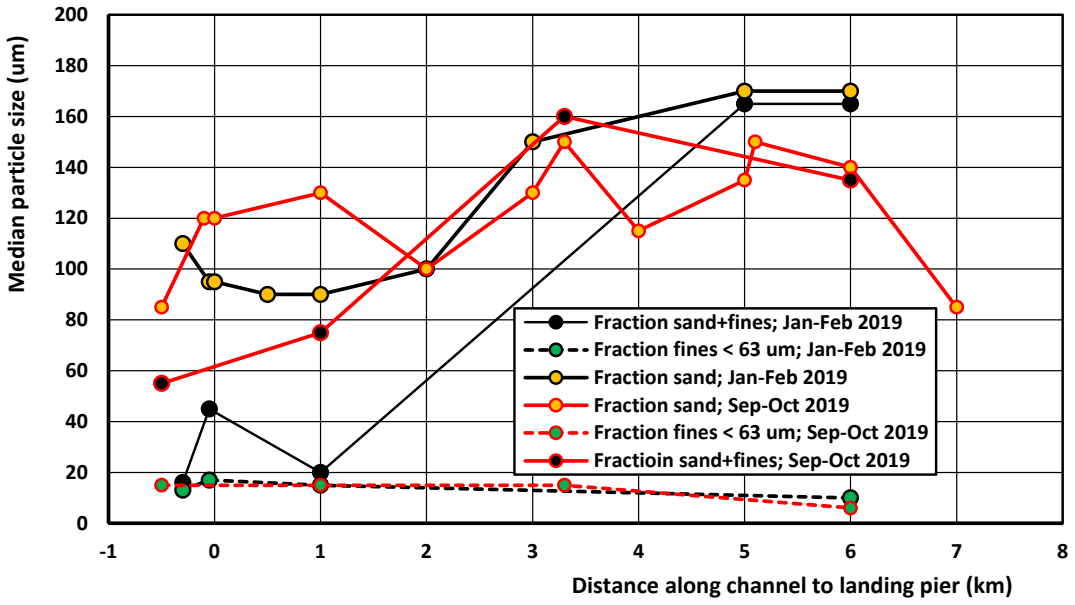

Figure 8 Median particle size (d_{50}); Holwerd ferry channel

Table 3.3 Measured and computed dry density values; Holwerd ferry channel

Sample	Measured dry density (kg/m^3)	Percentage sand (%)	Percentage clay <8 μm (%)	Percentage silt 8-63 μm (%)	Percentage organic materials (%)	Predicted dry density (kg/m^3)
1; KP10.4	1278	95	0	4	0	1552
2; KP9.2	1467	98	0	2	0	1584
3; KP9.0	1464	96	0	3	0	1570
4; KP8.5	1442	97	0	3	0	1576
5; KP9	1483	99	0	1	0	1592
6; KP7.5	1391	97	0	3	0	1576
7; KP5.8	1538	98	0	2	0	1584
8; KP3.3	732	17	23	60	5	805
9; KP2.8	1084	73	7	20	2	1328
10; KP2.4	1070	72	7	21	2	1320
11; KP1.5	1114	78	5	17	2	1375
12; KP0.9	1167	77	4	19	2	1372
13; KP0.3	1236	64	8	28	3	1240
14; KP0	992	49	12	39	3	1110
15;KP-0.6	1159	73	7	20	2	1328
16;KP-0.1	577	24	18	58	5	874

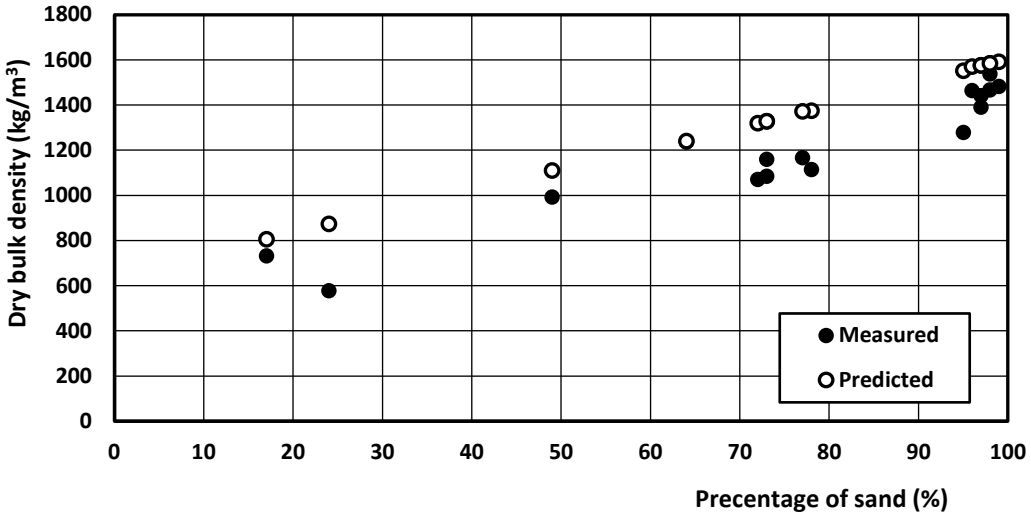

Figure 9 Measured and computed (Van Rijn and Barth, 2019) dry density values; Holwerd ferry channel

3.3 Sediment concentrations and transport

The sediment transport results were analyzed and critically compared with other measurements and to sediment transport predictors. First we show the measurement campaign results (3.3.1) followed by a preliminary analysis of the measured sediment concentrations and hydrodynamic conditions (3.3.2) and then we compare the measured results with sediment transport predictors (3.3.3) for sand and mud.

3.3.1 Measurement results

The four days of the measurement campaign included the desired hydrodynamic and bed composition conditions. The 4 chosen sites along the Holwerd channel offered a range between 10% of mud to 54% of mud, near bed flow velocities up to 1.5 m/s (day 2) and sediment concentrations up to range of 6-10 kg/m³ and even higher values (>20 kg/m³) which were induced by the passage of boats.

Each measurement day started at high tide slack water (Figure 10) and focused on the transition from ebb to flood when the maximum flow velocities occur. Here we show the results from Day 4 to represent the overall observed trends while the complete data from all measurements days are presented in the Appendix A. Figure 11 shows the near-bed flow velocity evolution over the tidal cycle at the location of Day 4. Due to the morphological configuration of the Wadden Sea with higher (inter- supratidal) mud flats and confined channels, the high water slack tide has longer duration while the low water slack tide is rather short or absent in the Holwerd channel. The peak ebb-flood velocities were rather similar to each other, as follows:

- Day 1: maximum flood velocity ≅ 0.7 m/s;
- Day 2: maximum ebb velocity ≅ 1.5 m/s; maximum flood velocity ≅ 1.4 m/s;
- Day 3: maximum ebb velocity ≅ 0.9 m/s; maximum flood velocity ≅ 1.1 m/s;
- Day 4: maximum ebb velocity ≅ 1.0 m/s; maximum flood velocity ≅ 1.05 m/s.

Exceptionally high velocities up to 1.5 m/s were measured on Day 2 at a location close to the new short-cut ferry channel (Figure 2), which was dredged in 2019. Such high velocities were not measured at that location during the field campaigns of 2019 (see Appendix B) before the dredging of the short-cut channel.

The sediment concentrations, both in terms of sand and mud, responded with a short time-lag to the flow velocities. The highest sediment concentrations were observed just after the peak of ebb on Day 4 (see Figure 12, Figure 13 and Figure 14). The sand concentrations respond in quasi-equilibrium with the flow velocities due to local resuspension while the mud concentrations are also controlled by advection. Nonetheless, the mud concentrations also respond strong to the flow velocity around the peak tidal discharges. The ebb phase shows higher mud concentration values on Day 2 with rather high maximum velocities of about 1.5 m/s when draining the muddy flats from the Wadden Sea in comparison with the lower mud concentrations during flood when the marine contribution is dominant. However, the sediment

concentrations along the Holwerd channel are also affected by dredging and dumping activities and the maritime traffic including the ferry between Holwerd and Ameland (see boat traffic at Appendix A). The dredging material is discarded between kp 3 and 4 (Figure 1) during ebb phase. Part of this material may be recirculated and come back during the following flood tidal phase. Most likely the sediment concentrations on Day 3 and 4 are higher during the flood phase due to the dredging activities despite the fact that the flow velocities were slightly lower during flood in comparison with ebb.

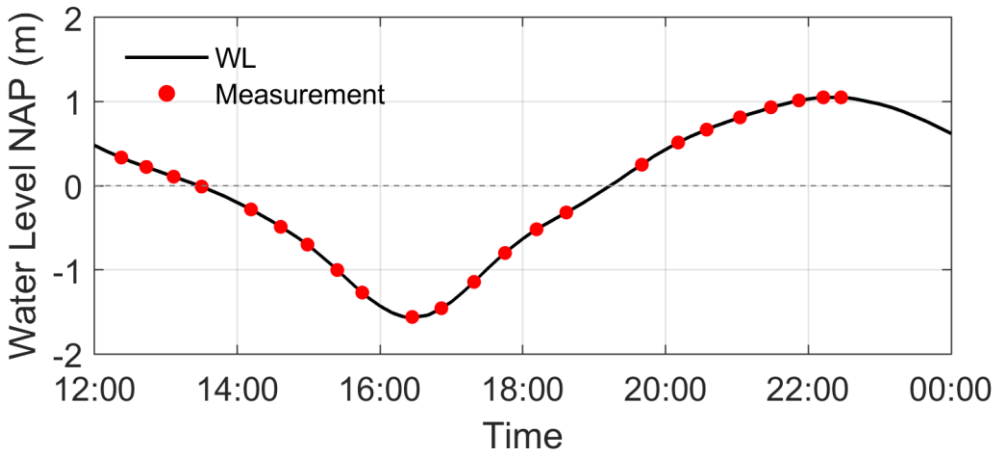

Figure 10 Tidal water levels and sampling times on Day 4; 15 June 2022.

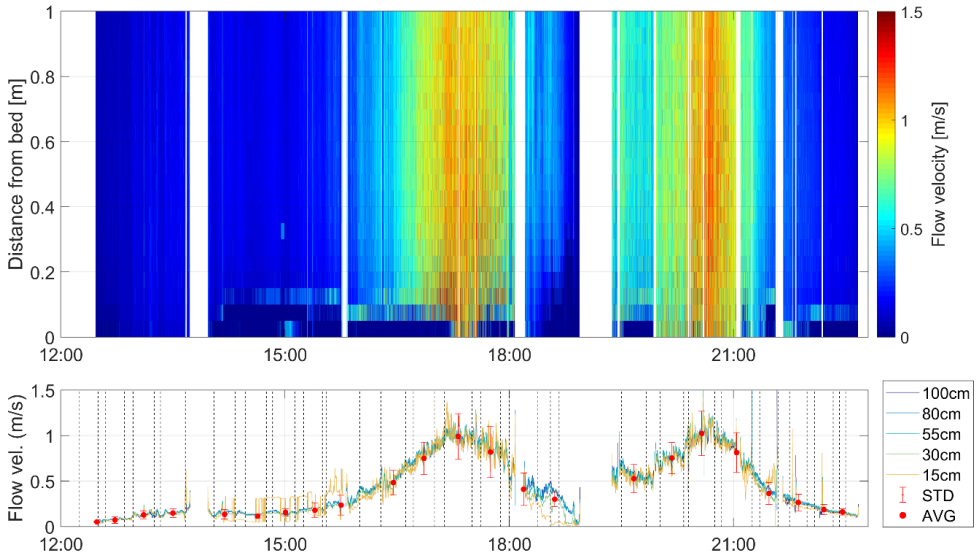

Figure 11 Near bed flow velocities measured by the ADCP on Day 4; 15 June 2022. Top panel: Velocity profile over the last 1m of water column towards the bed. Lower panel: Velocity over discrete heights from the bed and the corresponding average value within each measurement cycle.

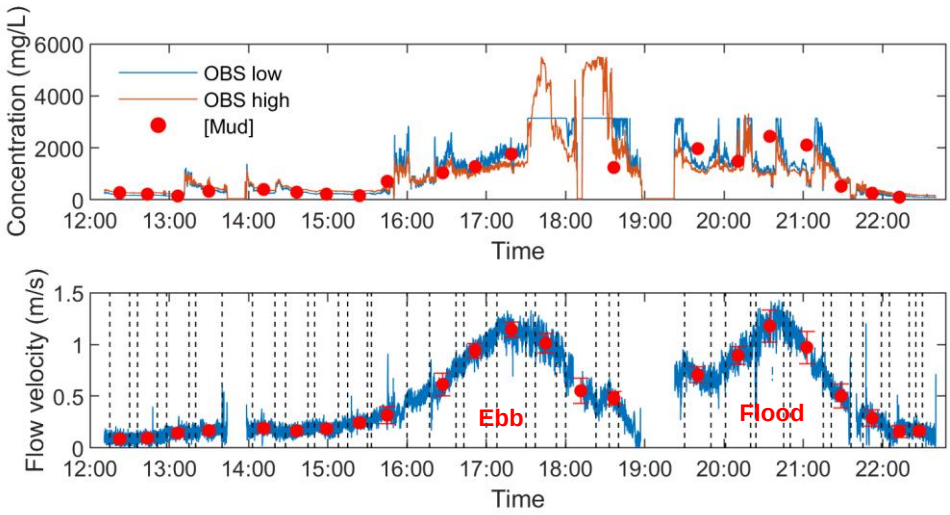

Figure 12 Depth-averaged current velocities and mud concentrations on Day 4; 15 June 2022. Top panel: OBS-sensor data for SSC, including both low and high range versus the measured mud (only) concentrations. Bottom panel: Aquadopp velocity data and the average flow velocity for each measurement cycle.

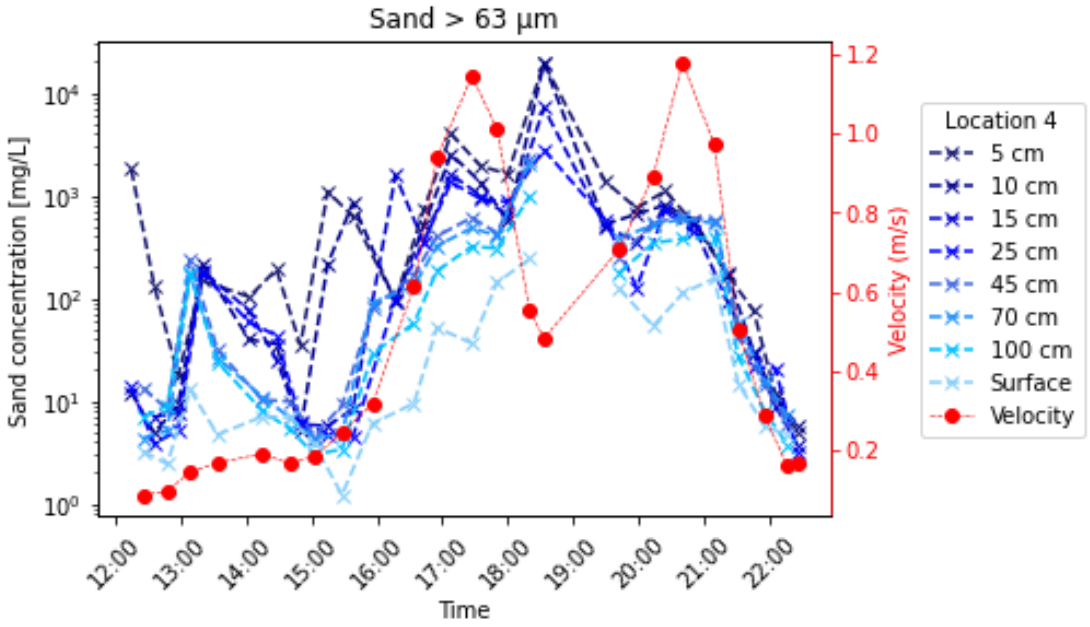

Figure 13 Measured sand concentrations at various elevations above the bed and depth-averaged current velocity over tidal cycle; Day 4; 15 June 2022

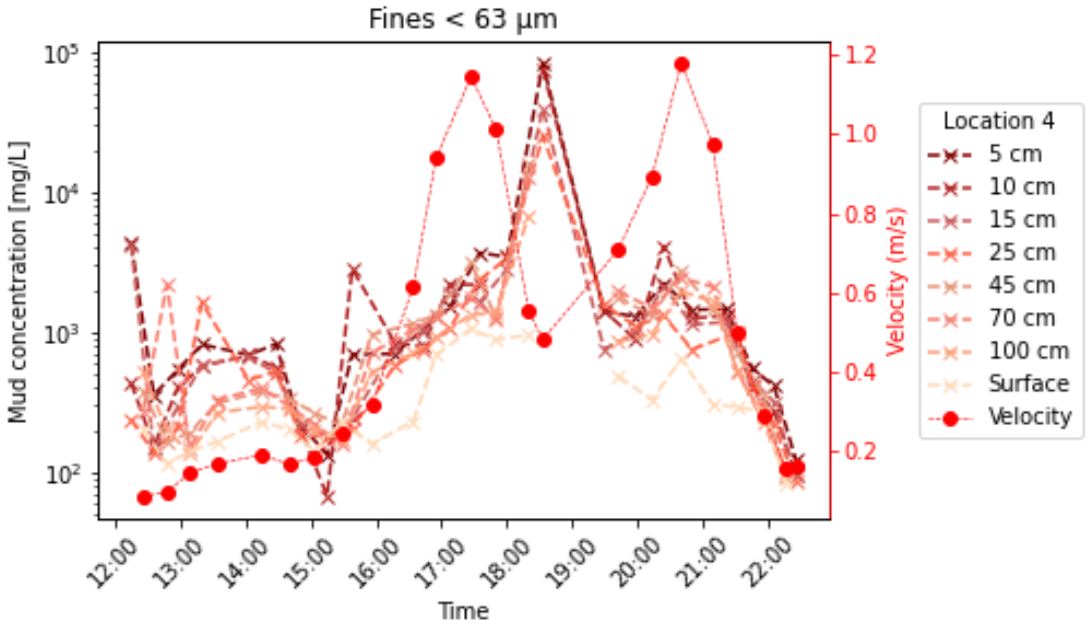

Figure 14 Measured mud concentrations (fines< 63 µm) at various elevations above the bed and depth-averaged current velocity over tidal cycle; Day 4; 15 June 2022

In general, the depth-averaged mud concentrations during the 4 measurement days, with values in the range of 500 to 1000 mg/l around peak flow velocities, are very similar to the values measured during the previous field campaigns in 2019 (Appendix B).

Table 3.4 Measured sand concentrations over the water depth. w/d= wet/dry bulk density

Dates	P_{fines}/P_{sand}(%) $d_{50,sand}$ (µm) w/d (kg/m³)	Peak tidal current (m/s)	Maximum concentrations Sand>63 µm (mg/l)			
			Layer<0.2m	0.2-0.5 m	0.5-1 m	surface
Day 1	27/73 140 1735/1160	Ebb: nd Flood: 0.8	no data 1000/2500	no data 200/1000	no data 50/200	no data 30/50
Day 2	10/90 120 1795/995	Ebb: 1.6 Flood: 1.5	2500/3500 1000/2000	1000/2500 300/1000	200/1000 100/300	100/200 50/100
Day 3	54/46 80 1505/890	Ebb: 0.9 Flood: 1.1	1000/3000 2000/20000	500/1000 500/1000	100-500 100-500	50/100 50/100
Day 4	34/66 120 1520/710	Ebb: 1.1 Flood: 1.15	1000/3000 500/1000	400/1000 400/1000	200/400 200/400	100/200 100/200

Table 3.5 Measured mud (fines< 63 µm) concentrations over the water depth. w/d= wet/dry bulk density

Dates	P_{fines}/P_{sand}(%) $d_{50,sand}$ (µm) w/d (kg/m³)	Peak tidal current (m/s)	Maximum mud concentrations Fines <63 µm (mg/l)			
			Layer <0.2m	0.2-0.5 m	0.5-1 m	surface
Day 1	27/73 140 1735/1160	Ebb: nd Flood: 0.8	no data 3000/8000	no data 500/3000	no data 200/500	no data 200/300
Day 2	10/90 120 1795/995	Ebb: 1.6 Flood: 1.5	4000/6000 2000/3000	2000/4000 1000/2000	1000/2000 500/1000	300/1000 200/500
Day 3	54/46 80 1505/890	Ebb: 0.9 Flood: 1.1	3000/6000 4000/20000	2000/3000 1000/2000	1000/2000 500/1000	300/1000 200/500
Day 4	34/66 120 1520/710	Ebb: 1.1 Flood: 1.15	2000/4000 2000/4000	1000/2000 1000/2000	500/1000 500/1000	300/500 300/500

The measured concentration data in the vertical layers between z=0.05 and 1 m above the bed have been combined to summarize the sand and mud concentrations in 5 (depth-averaged) velocity classes: v=0.5, 0.7, 0.9, 1.2 and 1.5 m/s (see Figure 15). The available concentrations at each sampling point above the bed were clustered and averaged within each velocity class. The error band width of each concentration profile is of the order of ±50%.The near-bed sand concentrations at z=0.05 m above the bed are approximately a factor of 5 higher than the values at z=1 m above the bed; the near-bed mud concentrations are also a factor of 5 higher than the values at 1 m above the bed (see Figure 15). This vertical difference of sediment concentrations near the bed shows the importance of detailed near-bed measurements in order to characterize sediment transport dynamics.

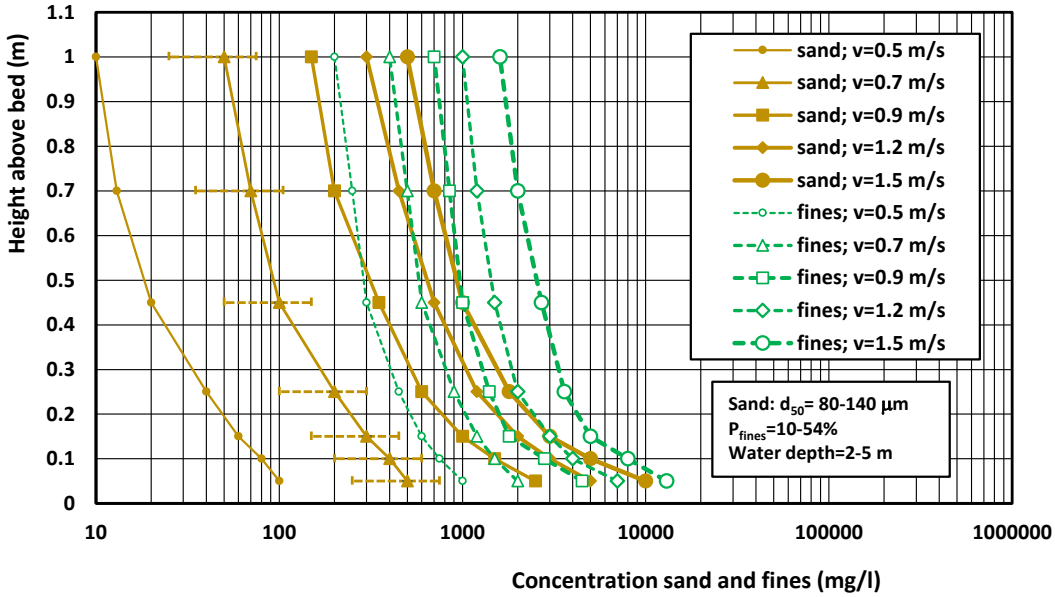

Figure 15 Measured sand and mud (fines) concentrations for 5 velocity classes v=0.5 to 1.5 m/s

The continuous measurements at Holwerd were challenging especially during low water conditions because of the combination of high flow velocities (>0.8 m/s) in the very narrow channel together with the passage of large vessels such as the Ameland ferry (Figure 16). The passage of such a large vessel in a narrow and shallow confined channel required the lifting of the frame and anchors for navigation safety. Similarly, the location of Day 2 at the channel bend formed a natural eddy and whirlpool (Figure 16) near the end of the ebb phase that forced the relocation of our boat until the conditions were normalized. Lastly, Day 1 location was composed of shallow and soft mud that did not allow for anchoring and a stable frame placement. For these reasons, there is a data gap near low water, and the measurement at Day 1 were limited (see Appendix A).

Figure 16 Holwerd channel. Left: Ameland ferry passing near the Bumblebee during low water. Right: Natural eddy/whirlpool that formed near the channel bend at Day 2 near low water.

3.3.2 Analyses of measured sediment transport

The mud and sand concentration data have been used to derive the depth-integrated mud and sand transport by integration over the depth. The lowest measurement point is at z=0.05 m above the bed. The mud and sand concentrations at the bed (z=0) are assumed to be equal to the values measured at z=0.05 m. The velocity at the bed is set to 0. Similarly, the mud and sand concentrations (and also the current velocity) at the water surface are assumed to equal to the values at the highest measurement point (just below the surface). The velocity profiles between the lowest and highest measurement points are assumed to have a logarithmic distribution.

Analysis of the transport rates shows that the depth-integrated sand transport responds fast to the changes in the depth-averaged current velocity at Day 1, 2 and 3 (see data in Appendix). The sand transport data of Day 4 show a short time delay (erosion lag) of about 1 hour during flood, see Figure 13.

The depth-integrated mud transport also responds strongly to the flow conditions. As an example, Figure 17 shows the depth-integrated mud transport over the tidal cycle of Day 3 (muddy location near Holwerd). The tidal variation of three mud concentrations is also shown. The main results of this plot for Day 3 are:

- peak flood velocity is slightly higher than the peak ebb velocity;
- near-bed mud concentration varies in the range of 1,000 to 30,000 mg/l; value is highest at peak flood flow;
- mud concentrations at 1 m above the bed during ebb flow are highest (order of 2000 mg/l) shortly after peak ebb flow and around peak flood flow;
- mud concentrations near the bed go back to values of the order of 1000 mg/l during slack tide; mud concentrations at 1 m above bed and near the water surface go back to values of 200 to 400 mg/l during slack tide.

Figure 18 shows the depth-integrated mud transport as function of the depth-averaged velocity for Day 3 and the other days (Day 1, 2 and 4). Measurable mud transport values occur down to a velocity of about 0.1 to 0.2 m/s due to the settling lag effect of fines. The depth-integrated mud transport during the Holwerd measurements can related to the current velocity ($q_{mud} \cong 2\ u_{mean}^2$). Most mud transport values are within a factor of 2 of the trendline. The mud transport rates during the flood period are somewhat higher than during the ebb period on Day 3 and 4 when the peak flood velocity is highest, while the mud transport during ebb is higher on Day 2 when the peak ebb velocity is highest. Natural hysteresis effects in the mud concentrations seems to be smaller compared to the dredging activities that exert a strong control on the flux of fine sediments along the channel. It is noted that one mud concentration profile with exceptionally high values near the bed in the range of 20 to 100 kg/m^3 at t=18.30 hours of Day 4 in conditions with a depth-averaged velocity of 0.6 m/s (about 1 hour after peak flow conditions, see Appendix) has been disregarded for the sediment transport analyses. This extreme measured sediment concentration was caused by the close passage of ferry boat (see boat passage at Appendix B) in combination with the high flow velocities just after low water. Although, it is important to acknowledge the strong effect of the maritime traffic in mobilizing sediments along the Holwerd channel.

In general, higher ebb concentrations are expected given the draining and erosion of the muddy flats from the Wadden Sea in comparison with the lower mud concentrations during flood when the marine contribution is dominant. However, the flood concentrations near Holwerd are also affected by dredging activities and maritime traffic.

Earlier sediment transport measurements from 2019 at Holwerd (Annex B) show similar mud transport values in the range of 0.5 to 3 kg/m/s (Figure B5, Appendix B) and the depth-integrated mud transport during flood and ebb are similar, likewise.

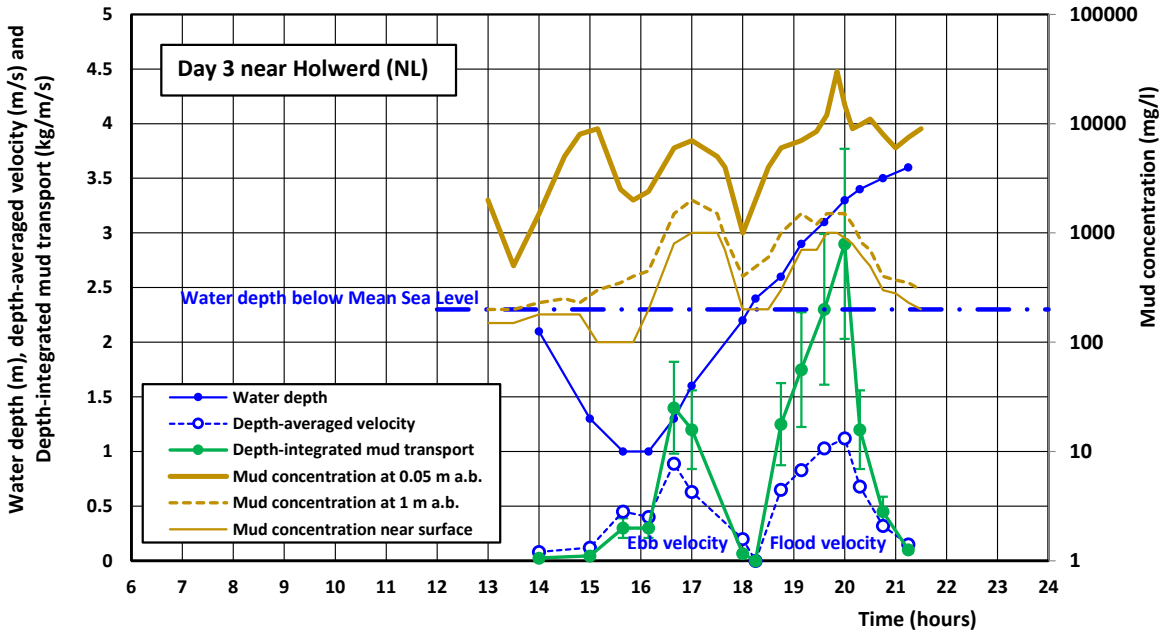

Figure 17 Depth-integrated mud transport during the tidal cycle, Day 3 near Holwerd

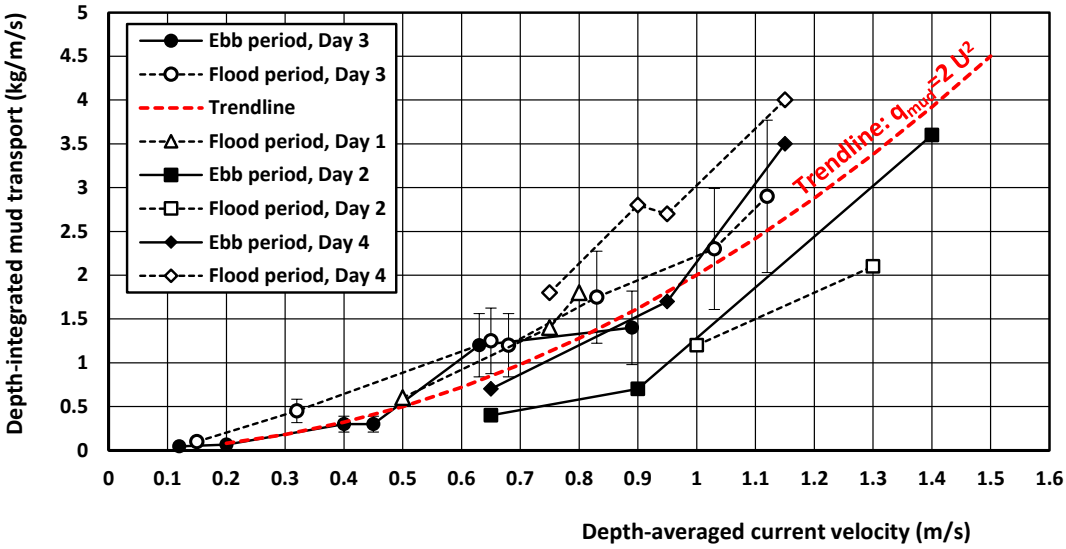

Figure 18 Depth-integrated mud transport as function depth-averaged velocity near Holwerd

The depth-integrated sand and mud transport are based on the trend lines of all data are shown in Table 3.6 and in Figure 19. The depth-averaged sand and mud concentrations have been computed as:

$c_{m,sand}=q_{s,sand}/(u_m\ h)$

$c_{m,mud}=q_{s,mud}/(u_m\ h)$

with

u_m=depth-averaged flow velocity,
h=water depth=4 m.

The results are given in Table 3.6 and in Figure 20. Measured sediment concentrations and transport of fine sediments (error bands of ±50%) in the coastal zone of Bengal Bay (Van Rijn 2021) are also shown for comparison.

The analysis of the results shows:

- sand and mud transport show strong response to the depth-averaged flow velocity;
  - the sand transport can be represented by: $q_{s,sand}=0.7\ u_m^{4.5}$;
  - the mud transport can be represented by: $q_{s,mud}=2\ u_m^{2}$;
  - NB. these empirical mud and sand transport functions are specifically valid for flow velocities >0.7 m/s around peak flow conditions at the site of Holwerd with sandy-mud bed (coarse silt bed) and are most likely time-site specific. We do not recommend further usage of these values.
- mud transport is a factor 10 higher than sand transport at low flow velocity of 0.5 m/s and factor 1.3 higher at high velocity of 1.5 m/s. The sand concentrations decrease more rapidly to low flow velocities around slack tide than the mud concentrations due to settling lag effects of mud;
- depth-averaged sand concentrations are in the range of 15 to 600 mg/l for velocity between 0.5 and 1.5 m/s; depth-averaged mud concentrations are in the range of 150 to 1000 mg/l for velocity between 0.5 and 1.5 m/s;
- the mud and sand concentrations at Holwerd are rather similar to those measured at the muddy-silty coastal zone of Bengal Bay, particularly at higher flow velocities > 1 m/s.

The depth-integrated mud transport values of the field campaigns in 2022 in the velocity range <1 m/s are in the same range as those of field campaigns in 2019 (Appendix B). Although, the sand transport values from 2022 are higher. This increase in sand concentration can be attributed to the change in the ferry channel configuration or to the fact that the sampling points in the 2022 campaign were collected closer to the bed where the sediment concentration are higher.

Table 3.6 Measured depth-integrated sand, mud transport and depth-averaged sand, mud concentrations

Flow velocity class (m/s)	Depth-integrated sand transport (kg/m/s)	Depth-integrated mud transport (kg/m/s	Depth-averaged sand concentration (mg/l)	Depth-averaged mud concentration (mg/l)
0.2	-	0.1	-	170
0.3	-	0.2	-	220
0.4	-	0.35	-	300
0.5	0.025	0.5	15	330
0.7	0.15	1.0	55	500
0.9	0.55	1.6	150	600
1.2	1.7	2.9	335	800
1.5	3.5	4.5	585	1000

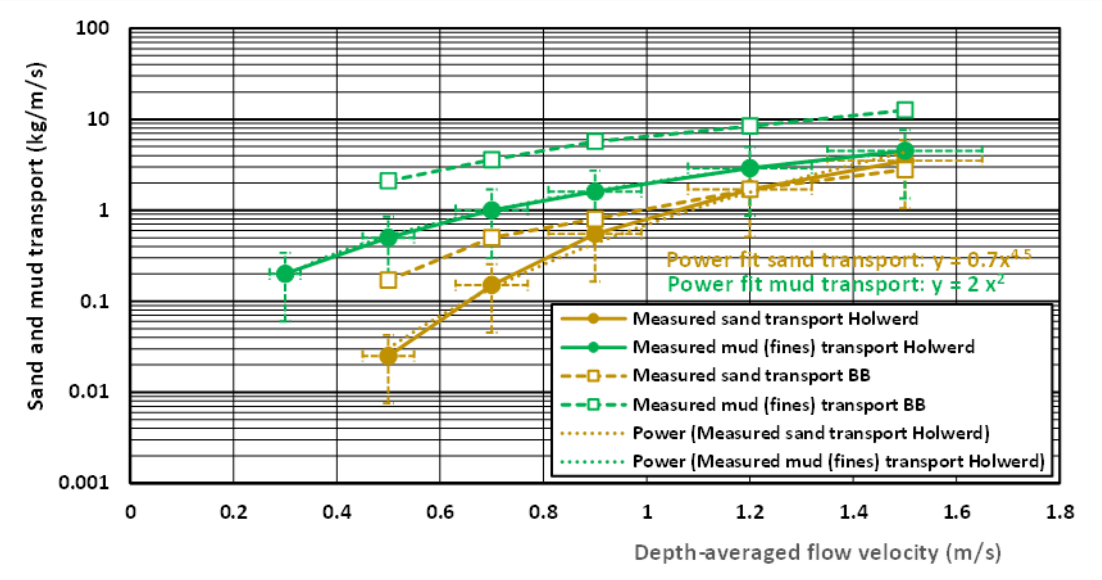

Figure 19 Depth-integrated sand and mud transport as function of depth-averaged flow velocity. BB = Bengal Bay data.

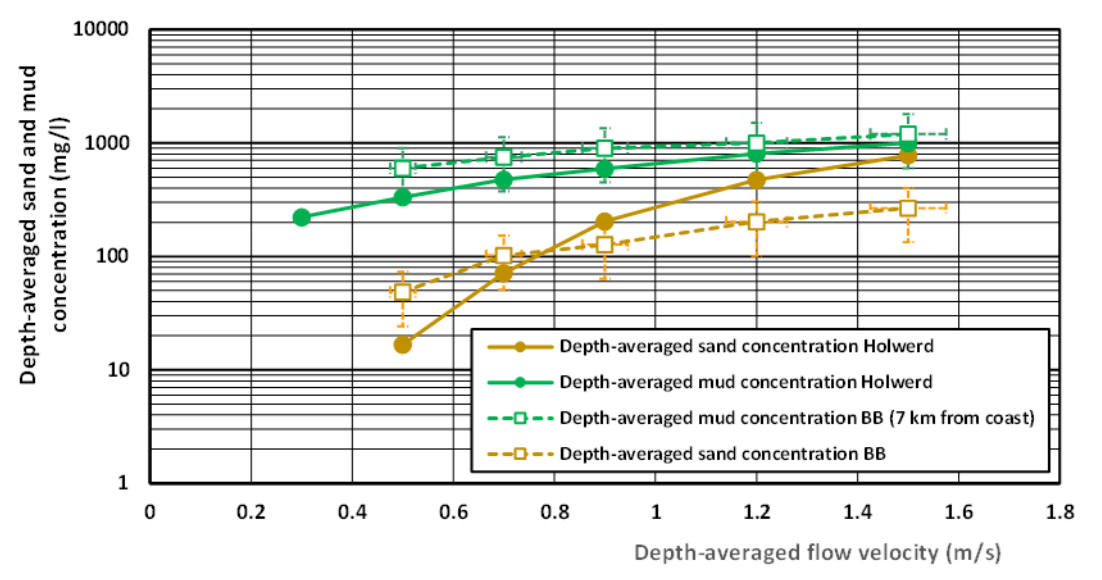

Figure 20 Depth-averaged sand and mud transport as function of depth-averaged flow velocity. BB = Bengal Bay data.

3.3.3 Modelling of sand and mud transport

The measured hydro-sediment data collected at Holwerd was compared and critically analyzed with two sediment transport models; namely, the sand transport of Van Rijn (2007) and the TMud transport of Van Rijn (2007; 2015).

3.3.3.1 Sand transport model of VR2007

The sand transport model of Van Rijn (2007) has been used to compute the sand concentration profiles based on the input data given in Table 3.4. The sand concentrations are computed numerically using 50 points over the water depth, and among other processes the model includes hindered settling and turbulence damping effects. The reference concentration near the bed is prescribed at a level of 0.05 m above the bed .The median sand diameter of the bed is set to 120 µm. The suspended sand is assumed

to be between 80 μm at low velocity (i.e. when finer sand particles are resuspended from the bed) to 120 μm at high velocity. The bed roughness is set to k_s=0.05 m at lower flow velocities when bed forms, such as ripples, are expected to form and to k_s=0.02 m at higher flow velocities when bed forms should be absent in higher mobility conditions (Van den Berg and Van Gelder, 1993). The water depth is set to h=4 m. Computations for a water depth of 3 m give similar values (within 30%),

Computed sand transport values are provided in Table 3.7 for two situations: (1) pure sand bed and (2) for mud-sand bed mixture with p_{fines}=0.3 (i.e. 30% mud). The damping of turbulent fluid motions is taken into account by using a damping factor acting on the fluid (momentum) mixing coefficient ($\varepsilon_s = \phi\ \varepsilon_f$ with $\phi=(1+2Ri^{0.5})^{-1}$ with Ri=flux Richardson-number related to the suspended sand particles; mud particles are excluded; ϕ-values < 1). The critical bed-shear stress of sand in a mixture with mud and sand is defined as: $\tau_{cr}=\tau_{cr,o}\,(1+p_{fines})$ and the sand concentrations and transport rate are multiplied with $(1-p_{fines})$ as part of the bed consists of muddy sediments.

The computed sand transport values are also shown in Figure 21 in comparison to the measured data at Holwerd. The computed values are higher for a pure sand bed (factor 3) and lower when the effect of the mud fraction, via Van Rijn (2007) method, is taken into account. The Van Rijn (2007) method including the effect of mud shows better agreement with the measured data than the results of the pure sand computation.

Figure 22 shows measured and computed sand concentration profiles for a pure sand bed (dashed curves) and mud-sand mixture with p_{fines}=0.3 (β = 1; dotted curves). In the latter case, the critical bed-shear stresses for erosion (τ_{crit}) of sand are higher resulting in lower near-bed concentrations due to the sediment pickup term (T) in Van Rijn (2007): $T=(\tau_c - \tau_{cr})/\tau_{cr}$. In general, the inclusion of mud cohesion effects improved the prediction of sand concentration, however, the predictions above 1 m/s are overestimated. The extra damping of turbulence due to the presence of the mud concentrations leads to less mixing of sand particles and thus to less steep sand concentration profiles in the near-bed layer. This effect is not yet taken into account in the sand transport model. As regards the β-factor in the equation $\tau_{cr}=\tau_{cr,o}\,(1+p_{fines})^{\beta}$, it is noted that a value of β = 1 produces the best agreement for field data, whereas a value of 2 gives better results for the flume data (see MUSA-Report 3 and 4; results of laboratory experiments; Phase 1A,B,C,D).

Table 3.7 Input data and computed sand transport. Temperature=15°C; Salinity=30 psu; Water density=1020 kg/m³; Sediment density=2650 kg/m³

Flow velocity class (m/s)	Water depth (m)	Wave height (m) peak period (s)	Bed sand $d_{50,bed}$ (µm)	Suspended sand $d_{50,sus}$ (µm)	Settling velocity (mm/s)	Bed roughness (m)	Computed depth-integrated sand transport (kg/m/s)	
							pure sand	sand & mud p_{fines}=0.3
0.5	4	0.2; 4	120	80	5.0	0.05	0.048	0.016
0.7	4	0.2; 4	120	90	6.3	0.04	0.25	0.10
0.9	4	0.2; 4	120	100	6.8	0.03	0.95	0.41
1.2	4	0.2; 4	120	110	8	0.02	4.5	2.0
1.5	4	0.2; 4	120	120	9.5	0.02	12.1	5.3

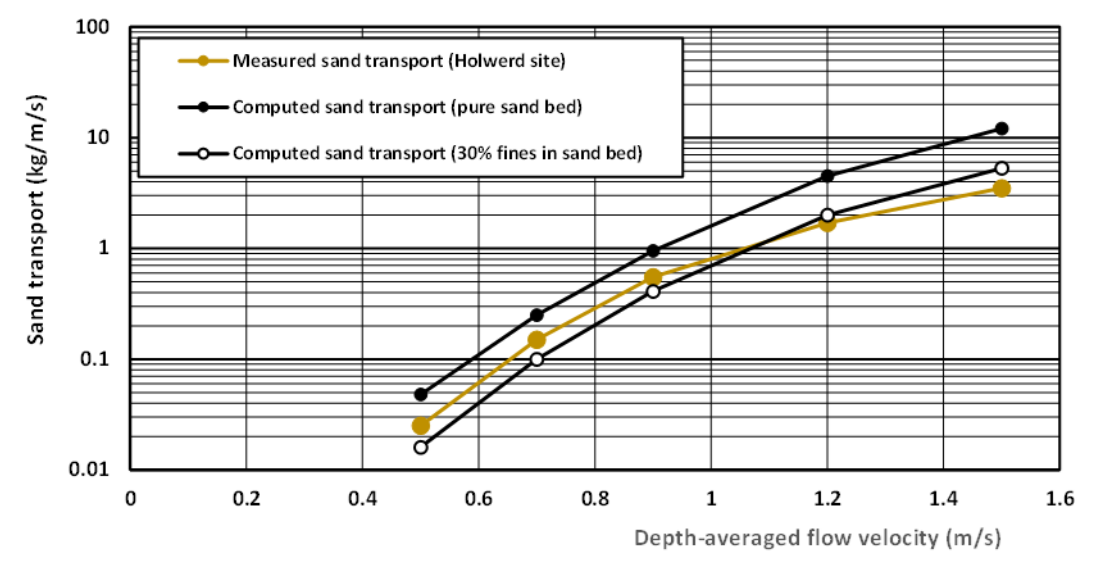

Figure 21 Measured and computed sand transport rates as function of depth-averaged flow velocity

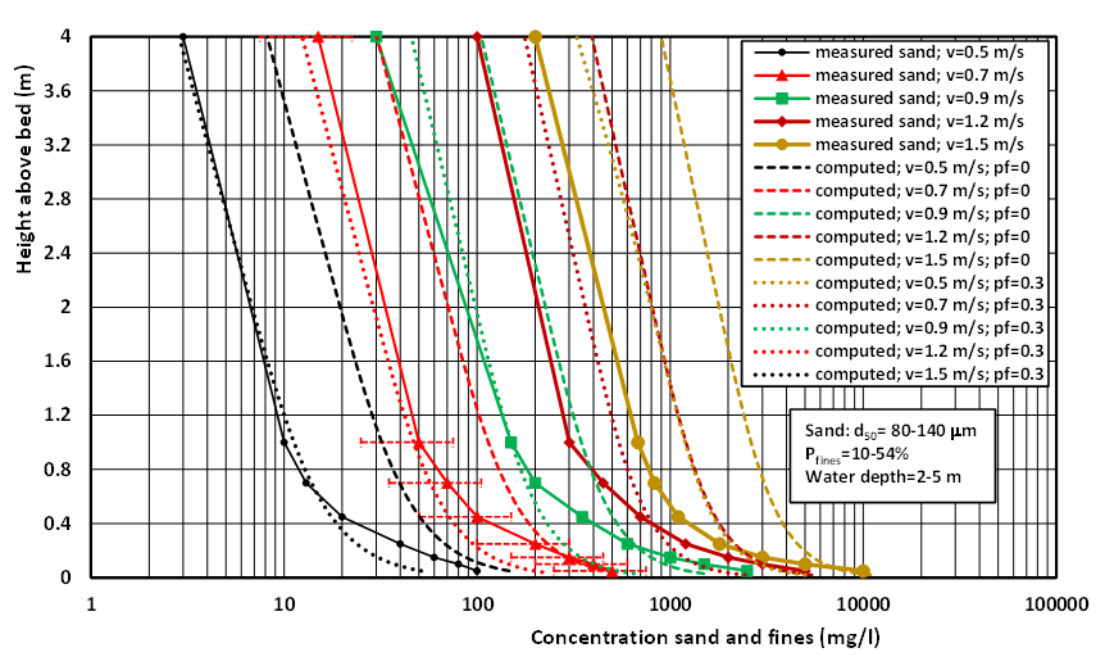

Figure 22 Measured and computed sand concentrations for 5 velocity classes v=0.5 to 1.5 m/s

3.3.3.2 Mud transport predictor

The TMUD-model (Van Rijn, 2007, 2015) has been used to simulate the transport of mud (including fluid mud) over the tidal cycle at the Holwerd site in the Dutch Wadden Sea .

Two situations were modelled and compared. First the conditions around the peak tidal flow of Day 3 (14 June 2023), see Figure 24. Second, the overall measurements from the 4-days campaigns, grouped as a function of flow velocities and associated mud concentrations. At the end we critically discuss the model limitations and the dependence on the settling velocity.

Process formulations

The time dependent 2DV advection-diffusion equation reads, as:

$$\partial c/\partial t + \partial(uc-\varepsilon_{s,x}\partial c/\partial x)/\partial x + \partial((w-w_{mud})c-\varepsilon_{s,z}\partial c/\partial z)/\partial z = 0$$

with: c= sediment concentration (volume), u, w= fluid velocities in x and z direction,

w_{mud}= settling velocity of mud, $\varepsilon_{s,x}$, $\varepsilon_{s,z}$ = sediment mixing coefficients in x and z direction,

x= longitudinal coordinate, z= vertical coordinate.

As the settling velocity and the sediment mixing coefficient are both dependent on the concentration, the 2DV advection-diffusion equation can only be solved numerically. The TMUD-model computes the mud concentration profile at each time over the tidal cycle representing the time-dependent term in a very approximate way. The vertical grid points are distributed over the water depth according to an exponential distribution resulting in very small grid sizes (millimeters) close to the bed where the mud concentration gradients are largest.

The vertical distribution of the velocity at each timestep *t* is represented by a logarithmic velocity profile above the fluid mud layer and a linear velocity profile inside the fluid mud layer (if present; no fluid mud layer at Holwerd site).

The boundary condition at the bed is represented by the reference bed concentration ($c_{a,mud}$ volume concentration):

$c_{a,mud}=p_{mud}\ \alpha_{mud}(\tau_{b,cw}-\tau_{b,cr,e})/\tau_{b,cr,e}$

with:

α_{mud}= erosion coefficient (input value; range of 0.001 to 0.003),p_{mud}= percentage of mud of top layer of bed, $\tau_{b,cr,e}$= critical bed-shear stress for erosion (input value), $\tau_{b,cw}$= $\tau_{b,c}+\tau_{b,w}$= bed-shear stress due to current and waves.

We acknowledge that the concept of a reference concentration is not entirely valid for a mud bed as there is typically no equilibrium condition between sedimentation and erosion near the bed, likewise in sandy beds. Here, the near-bed concentration may be limited by mud availability, for example. Nonetheless, the application of a reference concentration is a more practical approach that may be valid when a thick and uniform soft mud layer (i.e. recently deposited mud) is present on the bed which will act as a constant source of mud. This situation may be especially valid in mud-rich environments such as the Wadden Sea near Holwerd. Otherwise, the mud concentrations during high flow velocities are limited by the lower erosion rate of consolidated clay and subsurface hard layers.

The concentration-dependent mud settling velocity is represented in the TMUD-model as:

$w_{mud} = \exp[\alpha 1 \ln(c) + \alpha 2 - \alpha 3]$ for flocculation range $c \leq 0.0025$ ($\cong 7$ kg/m^3)

$w_{mud}= w_{mud,max}(1-c)^4$ for hindered settling range $c > 0.0025$

with:

$\alpha 1$ = $0.182 \ln(w_{mud,max}/w_{mud,min})$,
$\alpha 2$ = $2.09 \ln(w_{mud,max})$,
$\alpha 3$ = $1.09 \ln(w_{mud,min})$.
$w_{mud,max}$ = maximum settling velocity at c=0.0025,
$w_{mud,min}$ = minimum settling velocity at c=0.00001 ($\cong$0.025 kg/m^3).

The $\alpha 1$, $\alpha 1$ and $\alpha 3$-parameters have been derived from generic settling velocity data in estuaries (Van Rijn 1993) in a way to provide a gradual increase of settling velocities from $w_{mud.min}$ to $w_{mud,max}$ within the flocculation regime (see Figure 23). Using this approach, the settling velocity increases gradually for increasing mud concentrations (i.e. flocculation effect) up to a concentration value about 7 kg/m^3, and decreases for higher concentrations due to hindered settling effect. The settling velocity at height z_i is determined by using the concentration values at height z_{i-1}.

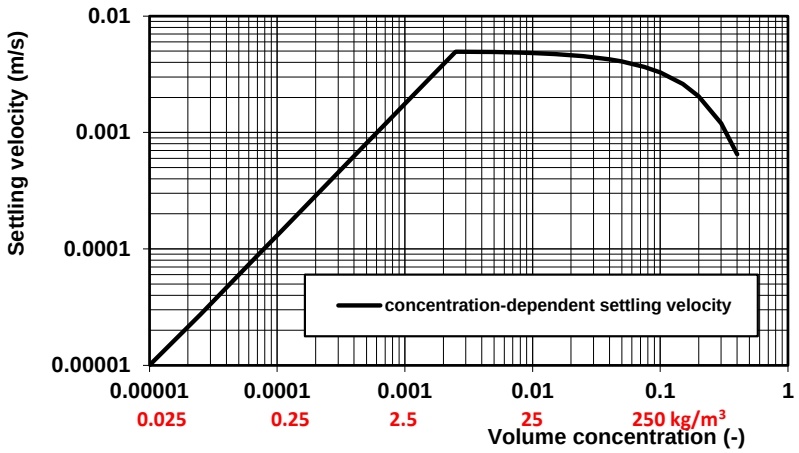

Figure 23 Computed mud settling velocity as function of mud concentration; $w_{mud,max}$=5 mm/s; $w_{mud,min}$=0.01 mm/s

The sediment mixing coefficient distribution over the water depth is represented by:

$\varepsilon_s= \phi_d\ \varepsilon_b$ for $z \leq \delta_{fm}$
$\varepsilon_s= \phi_d\ [\varepsilon_b + (\varepsilon_{max} - \varepsilon_b)\ (z-\delta_{fm})/(0.5h-\delta_{fm})]$ for $\delta_{fm} < z < 0.5h$
$\varepsilon_s= \phi_d\ [(h-z)/(0.5h)]\ \varepsilon_{max}$ for $z \geq 0.5h$
$\varepsilon_{max}= 0.05\ \gamma_{mix}\ u_{*,cw}\ h$
$\varepsilon_b= 0.5\ \varepsilon_{max}$

with:
δ_{fm} = thickness of high-concentration near-bed layer (input value in range 0 to 1 m),
ε_b= sediment mixing coefficient at top of high-concentration layer,
ε_{max}= maximum sediment mixing coefficient at z/h=0.5, h= water depth,
$u_{*,cw}= (u_{*,c}^2+u_{*,w}^2)^{0.5}$= bed-shear velocity due to current and waves,
$u_{*,c}= (\tau_{b,c}/\rho_w)^{0.5}$= current-related bed-shear stress,
$u_{*,w}= (\tau_{b,w}/\rho_w)^{0.5}$= wave-related bed-shear stress,
γ_{mix}= calibration coefficient (default=1),
ϕ_d= turbulence damping coefficient (function of Richardson number),
$Ri= [-(g/\rho)][d\rho/dz]/[(du/dz)^2]= [-(\rho_s-\rho_w)g/((\rho_w+(\rho_s-\rho_w)c)][dc/dz]/[(du/dz)^2]$ = Richardson number (salinity and temperature effects on the vertical density gradient are neglected),
ρ= fluid-sediment mixture density=$\rho_s c+(1-c)\rho_w$, c= volume concentration.

The concentration and velocity gradients are determined by using the values at heights z_{i-1} and z_{i-2}. The damping function is expressed as (Munk and Anderson 1948): $\phi_d=(1 + \alpha_d\, 2Ri^{0.5})^{-1}$ with: α_d= calibration coefficient (default=1; in range of 0 to 2), Ri=Richardson number (-).

It is noted that the numerical TMUD-model is a simple model for mud transport in tidal flow based on the quasi-steady computation of the mud concentration profiles largely neglecting the $\partial c/\partial t$-term of the 2DV advection-diffusion equation. The full time dependent 2DV-advection-diffusion equation is modelled by more sophisticated models (DELFT3D and SUSTIM (Van Rijn and Meijer, 2023).

Model boundary conditions and input data

The input data used for Day 3 at Holwerd are given in The velocities and mud concentrations are computed numerically (2DV) with 50 grid points according to exponential distribution over the depth (very small grid sizes of mm's near the bed).

Table 3.8. The maximum flood velocity is slightly higher than the maximum ebb velocity, see Figure A18.

The velocities and mud concentrations are computed numerically (2DV) with 50 grid points according to exponential distribution over the depth (very small grid sizes of mm's near the bed).

Table 3.8: Input data for the TMUD-model based on the measured data at Day 3 in ferry channel Holwerd (NL)

Parameter	Value	
Tidal range	2.4 m	
Water depth to mean Sea level (MSL)	2.3 m	
Peak tidal current velocity (depth-averaged Flood, Ebb)	1.1; 0.9 m/s	
Percentage of mud in the bed (p_{mud})	55%	
Maximum and minimum settling velocity ($w_{mud,\,max}$; $w_{mud,min}$)	5; 0.01 mm/s	
Critical bed-shear stress for erosion ($\tau_{b,cr,e}$)	0.2 N/m^2	
Thickness of high-concentration layer near bed surface (δ_{fm})	0.02 m	
Bed roughness (k_s)	0.02 m	
Reference level bed concentration (a)	0.02 m	

Calibration coefficient bed concentration (α_{mud})	0.002	
Turbulence damping coefficient related to sediment mixing (α_d)	2 (default 1)	
Calibration coefficient of sediment mixing (γ_{mix})	0.5 (default 1)	

Day 3 conditions

Figure 24 and Figure 25 show the computed and measured mud concentration profiles at maximum flow conditions at Day 3 (14 June 2022). The scaling coefficient (α_{mud}) of the near-bed concentration is set to match a bed concentration in the order of 5 kg/m^3. The bed concentration is computed at a level of a=0.02 m above the bed (at top of the high-concentration layer near the bed). Applying the variable settling velocity method, the settling velocity varies from 4 mm/s in the near-bed layer to about 0.17 mm/s near the water surface (Figure 23**)**. The agreement between computed and measured concentrations is satisfactory specially around the peak tidal flow conditions. Generally, the computed mud concentrations in the near-bed zone (0.1 to 1 m) are slightly higher than the measured values, and slightly lower in the zone near the water surface.

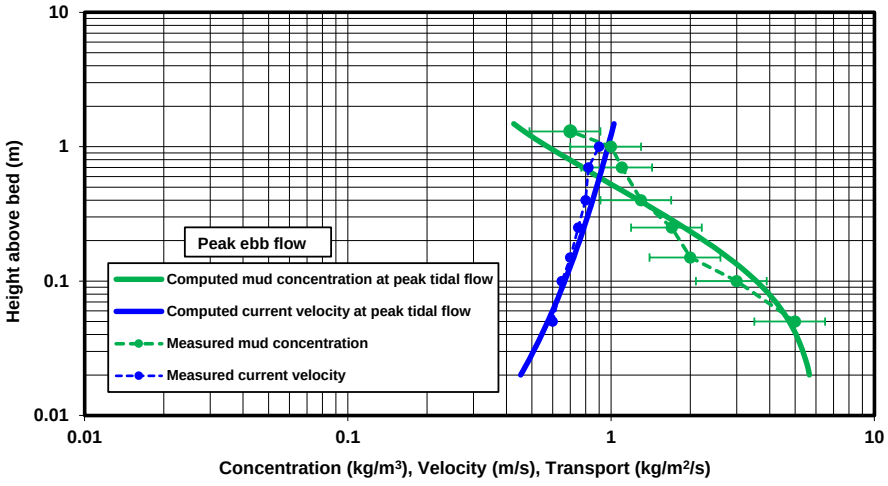

Figure 24 Computed mud transport at peak ebb flow; Day 3; 14 June 2022 near Holwerd (NL)

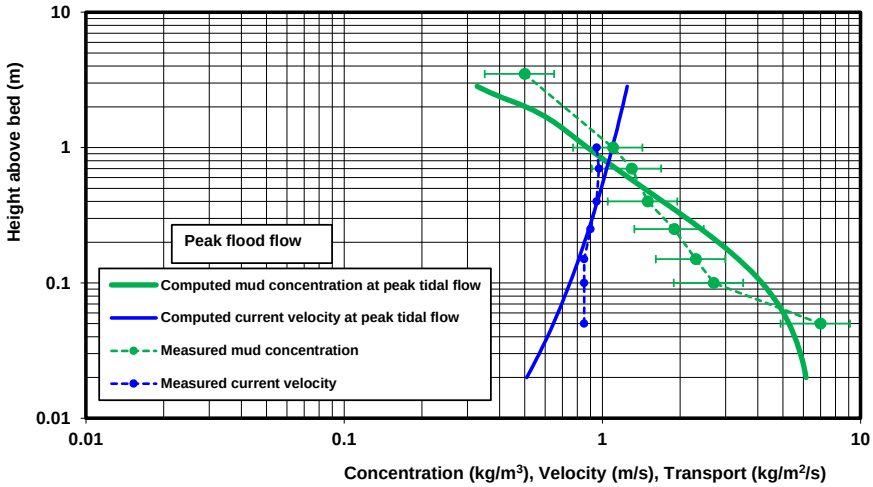

Figure 25 Computed mud transport at peak flood flow; Day 3; 14 June 2022 near Holwerd (NL)

Combined 4-days campaign

The TMud-model with the input settings of The velocities and mud concentrations are computed numerically (2DV) with 50 grid points according to exponential distribution over the depth (very small grid sizes of mm's near the bed).

Table 3.8 (current velocity extended to 1.5 m/s) has been used to expand the depth-integrated (equilibrium) mud transport to the entire 4-days campaign as function of depth-averaged tidal current velocity (Figure 26**)**. Horizontal advection effects are not included in the local equilibrium approach.

The computed (equilibrium) values show good overall agreement with the measured values (see Table 3.6) for current velocity values above 0.7 m/s. The computed values progressively lower for velocities below 0.7 m/s, up to factor of 10 for a velocity of 0.5 m/s (minimum computed velocity). It is noted that the tidal period with low current velocities below critical conditions for erosion (<0.4 m/s) is dominated by settling processes (settling lag effects), which is a slow process for very fine sediments with low settling velocities < 0.5 mm/s. For example, the settling time of sediments with settling velocity of 0.5 mm/s over a water depth of 3 m is about 6000 s (about 2 hours). Here, the mud settling lag processes around slack tide with low current velocities can not be modelled by a local, quasi-equilibrium approach, as assumed in the TMud-model. At high current velocities, the erosion and upward mixing is a much faster process (minor erosion lag) and dominated the resultant sediment concentrations, allowing a quasi-equilibrium assumption.

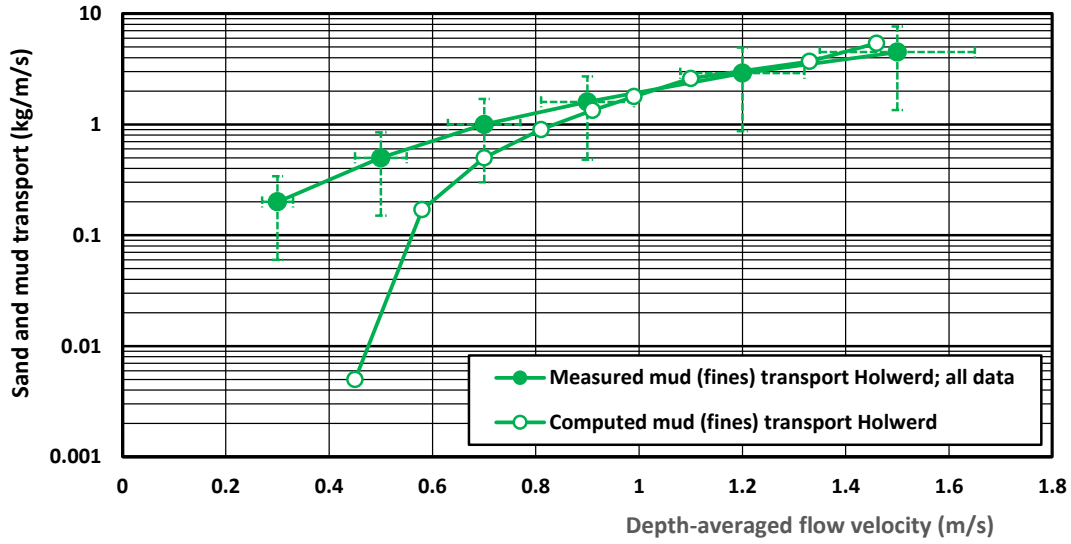

Figure 26 Measured and computed mud transport as function of depth-averaged velocity; Holwerd

Model dependency on free parameters

It is noted that the modelled mud concentrations deriverd from the TMud model is constrained by many free (calibration) parameters that affect, for example, the near-bed concentration, settling velocity and vertical mixing. Therefore, the model settings presented here are likely site-dependent. Thus, the model requires substantial calibration based on measured hydrodynamic and sediment concentration data. Further research and comparisons are required to study the generality of these parameters. However, the present model results show good agreement with the measured data at Holwerd under the current assumptions; for example, the equilibrium mud concentration and the variable settling velocity.

In order to illustrate the model dependency and response on the variation of the input (free) parameters, we performed simulations varying the mud settling velocity. Figure 27 shows the effect of a constant

settling velocity in the range of 0.1 to 5 mm/s on the computed mud concentration profile for peak flood flow conditions. Two plots are given with logarithmic and linear axes for visualization purposes. For a settling velocity of 5 mm/s, the mud concentrations are excessively low in the upper part of the water column when compared to the measured values. The mud concentrations are almost uniform over the depth for a settling velocity of 0.1 mm/s. Based on this, it is concluded that a concentration-dependent mud settling velocity is essential for a good representation of the measured mud concentrations at the Holwerd site, particularly when modelling with one sediment fraction. An alternative to the variable settling velocity is the approach with multiple sediment fractions (minimum 2 fractions) in which the sediment concentrations and (vertical) distribution are determined more by the model physics than by user-defined free parameters. However, the multi-fraction approach requires more detailed information about the sediment characteristics and usually results in longer computational times. Nonetheless, using multiple sediment fractions may be desirable as it involves more physics and less fitting and calibration. In any case, a concentration dependent settling velocity remains necessary to properly represent the flocculation and hindered settling processes.

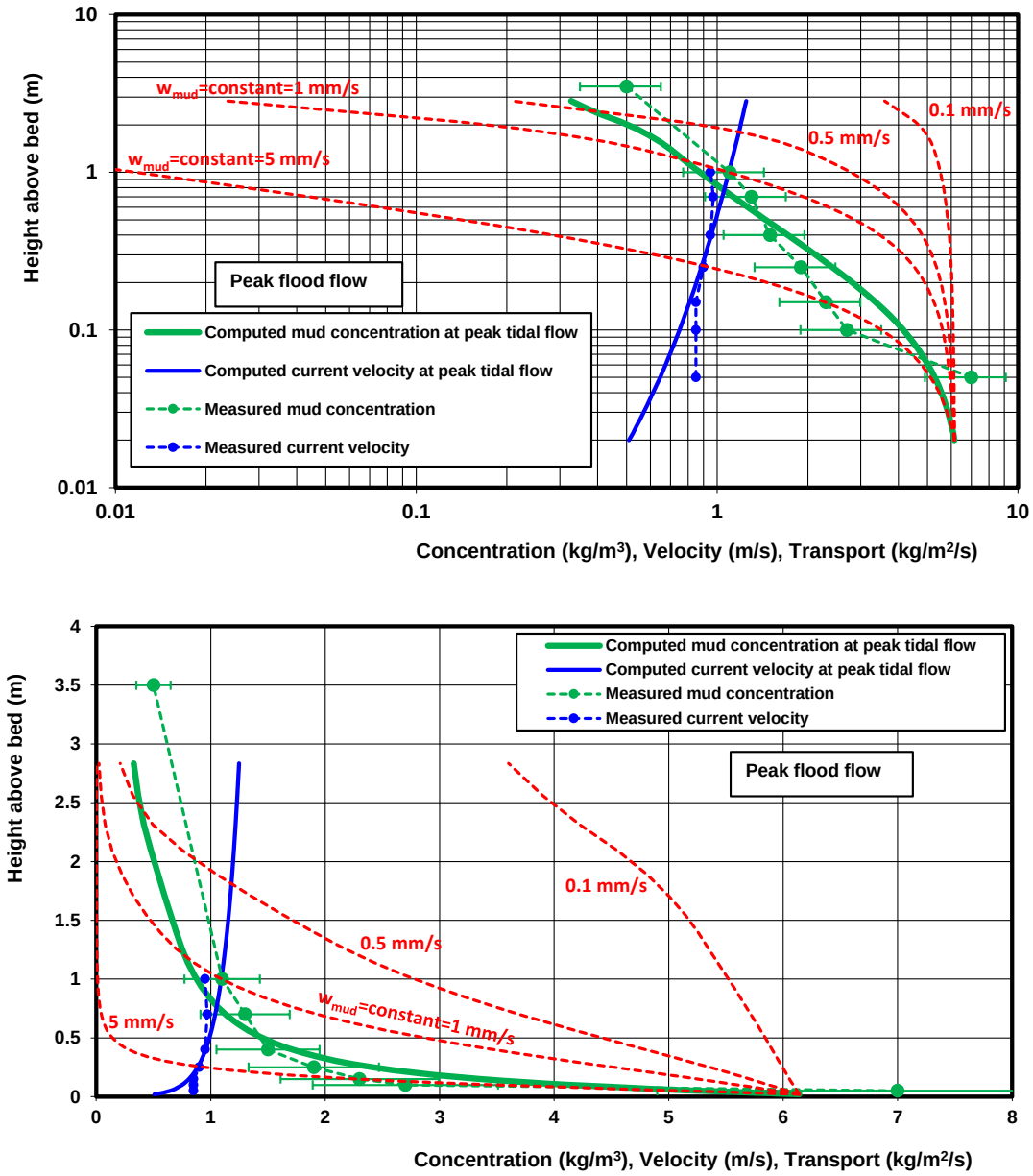

Figure 27 Effect of constant settling velocity on computed concentration profile at peak flood flow; Day 3 (Upper: logarithmic axis; Lower: linear axis)

4 Conclusions

Detailed near-bed hydrodynamic and sediment transport field measurements have been performed in the tidal ferry channel between Holwerd and Ameland in the Wadden Sea (NL) in May and June (4 days) of 2022.

The primary objective of the MUSA field campaigns during the 4 days measurements are: 1) to explore the novel measurement setup and procedures to measure flow velocities and mud and sand concentrations in the lowest 1 m of the water column with several instruments 2) to acquire sediment concentrations and sediment composition over distinct hydrodynamic conditions and bed compositions and to compare the results with theoretical formulations.

The main findings are, as follows:

- The Holwerd channel between Holwerd and Ameland shows a strong gradation from mud near the Holwerd ferry pier to sandy beds towards the Ameland Island. Our measurement sites comprised mud percentages between 10 and 54%.
- The peak flood and ebb flow velocities were rather similar to each other along the 4-days covering 4 different places along the channel. The peak velocities were in the range of 0.9-1.1 m/s with the maximum measured value of about 1.5 m/s.
- Mud concentrations at the Holwerd channel were higher during ebb on Day 2 with the highest peak ebb velocity when draining the muddy flats than during flood when marine water from the North Sea floods the tidal basin. Conversely, mud concentrations were somewhat higher during the flood phase on Day 3 and 4. It is important to note that mud concentrations during flood may be affected by recirculation effects due to the nearby disposal of dredged materials during the ebb phase.
- The sand concentrations responded in quasi-equilibrium condition with flow velocities, i.e. local resuspension, while mud concentrations were also influenced by advection, particularly, from the muddy flats, the North Sea and the dredging activities.
- The sand and mud (fines) concentrations are generally lower (100 to 1000 mg/l) in the period around slack tide with low velocities, e.g. lower than 0.5 m/s. Low water slack in the Holwerd channel is rather absent while high water slack is lengthy.
- The near-bed sand and mud concentrations are generally in the range of 1000 to 10,000 mg/l; the near-bed mud concentrations are about 2 to 3 times higher than the near-bed-sand concentrations (see Table 3.4, Table 3.5).
- Extreme mud and sand concentrations are in the range of 20,000 to 80,000 mg/l at 0.05 m above the local bed; these values are associated with the passage of boats especially around low tide. These extreme values highlight the effect of maritime traffic on the resuspension of sediments.
- The sediment transport equations of Van Rijn (2007) showed good agreement with the measured data in terms of sand concentrations. The best results were found when including the effect of mud in the critical shear stress of sand. However, at higher flow velocities, here 1 m/s, the computed values are somehow overestimated.
- The equilibrium-based mud transport near the peak flow velocities can be simulated rather well by using a diffusion type of equation (TMud-model; Van Rijn 2015) with concentration-dependent settling velocity and sediment mixing. The mismatches between modelled and measured values of mud concentrations can be mainly attributed to the mud settling lag around slack water conditions and to mud advection that is not accounted in the TMud model.

5 References

Van Den Berg, J.H. and Van Gelder, A. (1993). A New Bedform Stability Diagram, with Emphasis on the Transition of Ripples to Plane Bed in Flows over Fine Sand and Silt. In Alluvial Sedimentation (eds M. Marzo and C. Puigdefábregas). https://doi.org/10.1002/9781444303995.ch2

Van Rijn, L.C., 2007. Unified view of sediment transport by currents and waves, part 2: suspended transport. Journal of Hydraulic Engineering, ASCE, Vol. 133, No. 6

Van Rijn, L.C., 2015. Principles of erosion and sedimentation engineering in rivers, estuaries and coastal seas. www.aquapublications.nl

Van Rijn, L.C., 2021. Modelling of sediment deposition trial pits and shipping channel, Payra, Bangladesh (classified report)

Van Rijn, L.C. and Meijer, K.L., 2023. Modelling of sand and mud transport in tidal flow; SUSTIM2DV-model. LVRS-Consultancy, The Netherlands

Van Rijn, L.C. and Barth, R., 2019. Settling and consolidation of soft mud-sand layers. Journal Waterway, Port, Coastal, Ocean Engineering, ASCE, Vol. 145, No. 1: 04018028

A Data from Holwerd 2022

A.1 Boat passages

The passage of boat were manually annotated during the field campaign. Some boats may be missing in this list.

Day 1 – No boats passed because the measurement site was downstream (by the end of the channel) from the Holwerd Ferry Pier (see Figure 2).

Table A 1 Boat passages during the measurement campaign from Day 2: 17 May 2022

Time	boat type	Time	boat type
11:00	Ferry	13:30	Ferry
11:20	Fisher	14:22	big boat + ferry
11:25	survey	14:36	ferry
11:32	survey	14:49	big boat
11:38	small	15:18	ferry
11:43	survey	15:42	ferry
11:45	ferry	16:00	fast ferry
11:52	big boat	16:18	Ferry
11:58	zeehondenboot	16:23	big boat
12:30	fast ferry	16:25	fast ferry
13:05	ferry	17:01	fast ferry
13:08	fast ferry	20:10	Ferry
13:25	zeehondenboot	20:50	Ferry

Table A 2 Boat passages during the measurement campaign from Day 3: 14 June 2022

Time	boat type	Time	boat type
13:45	Ferry	16:37	small boat
14:12	Ferry	17:05	small ferry
14:41	Ferry	18:17	Ferry
15:05	Ferry	18:39	Ferry
15:51	water taxi	19:02	small ferry
16:03	small ferry	20:18	Ferry
16:11	Ferry	20:35	Ferry
16:33	ferry	21:07	small boat

Table A 3 Boat passages during the measurement campaign from Day 4: 15 June 2022

Time	boat type	Time	boat type
12:47	small boat	16:23	water taxi
13:07	Hopper dredger	18:05	ferry
13:07	fast ferry	18:44	fast ferry
13:40	ferry	18:56	ferry
14:10	ferry	19:05	small ferry
15:28	water taxi	19:57	rondvaart boot
15:36	water taxi	20:22	rondvaart boot
15:45	ferry	20:36	ferry
16:17	ferry	20:57	ferry
16:20	small ferry		

A.2 Data of Day 1-16 May 2022

The background data are given in Table A 4.

Table A 4 Background data; Day 1-16 May 2022

Location	1. East of the Holwerd harbour (53º23'50"N / 5º52'49"E)
Date	16 May 2022
Wind	4 Beaufort
Water temperature	16.4 ºC
Wave height/period (estimated)	No waves
Bed level to Datum (NAP)	3.25 m
Type of bed sediment, d_{50} sand fraction	140 um
Type of suspended sediment	fines < 63 μm and sand
Wet/Dry density of bed sample	1734;1159
Percentage sand of bed sample	73%
Percentage of shells	Mussels and shells in the sample, ca. 10%
Percentage of organic materials	Little < 3%
Bed form data	Not measured
Sinking of bed fish in bed	Location with very soft mud. The frame possibly sunk up to 15-20 cm and during strong flow the frame was not stable in position.

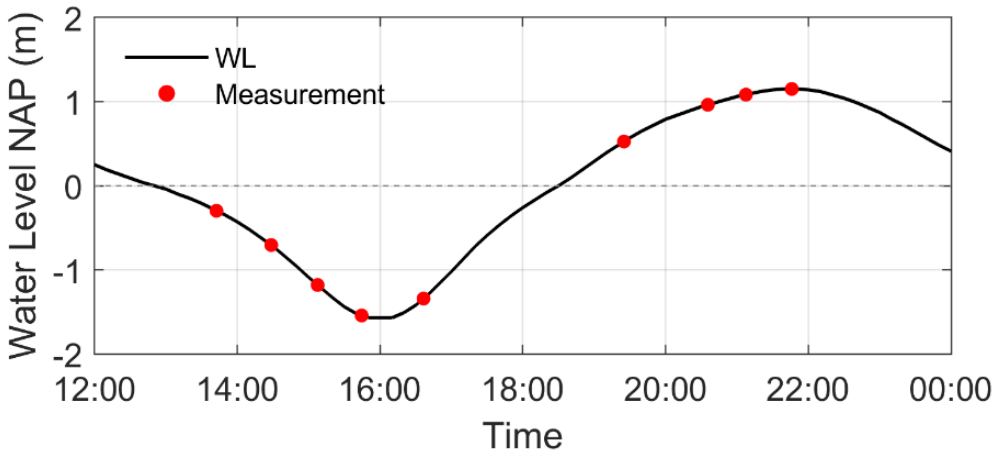

Figure A 1 Tidal water levels and sampling times on Day 1; 16 May 2022

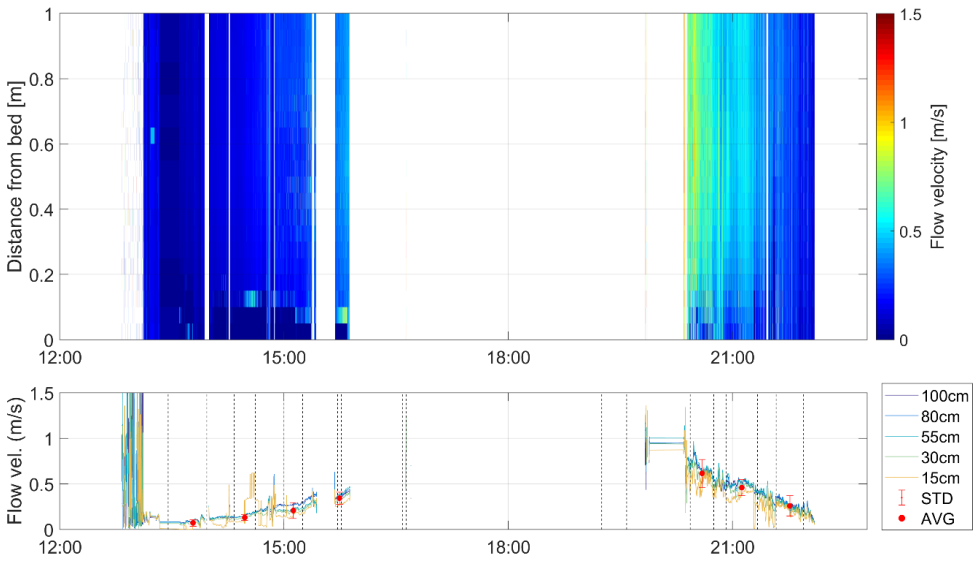

Figure A 2 Tidal current velocities on Day 1 based on ADCP-data; 16 May 2022 red dot= current velocity averaged over near bed-layer of 1 m

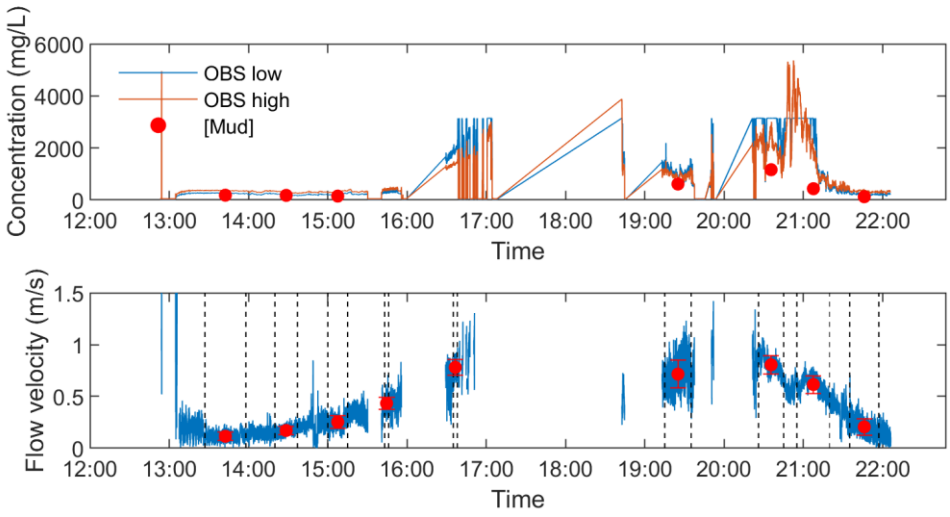

Figure A 3 Mud concentrations and current velocity on Day 1; 16 May 2022. Top Panel: Concentrations from samples [Mud] and OBS at 1 m above bed (low/high range instrument setting); red dot= average value of OBS-data; Bottom Panel: Aquadopp flow velocity at 1.2 m above bed; red dot=average value of flow velocity within a sampling cycle.

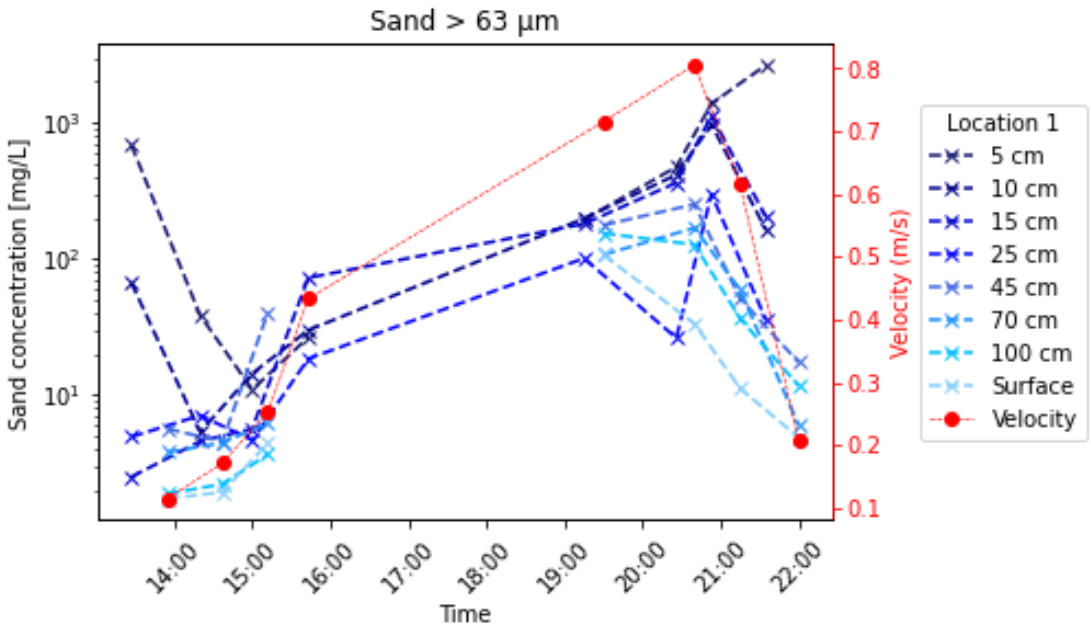

Figure A 4 Sand concentrations at various elevations above the bed and depth-averaged current velocity over tidal cycle; Day 1; 16 May 2022

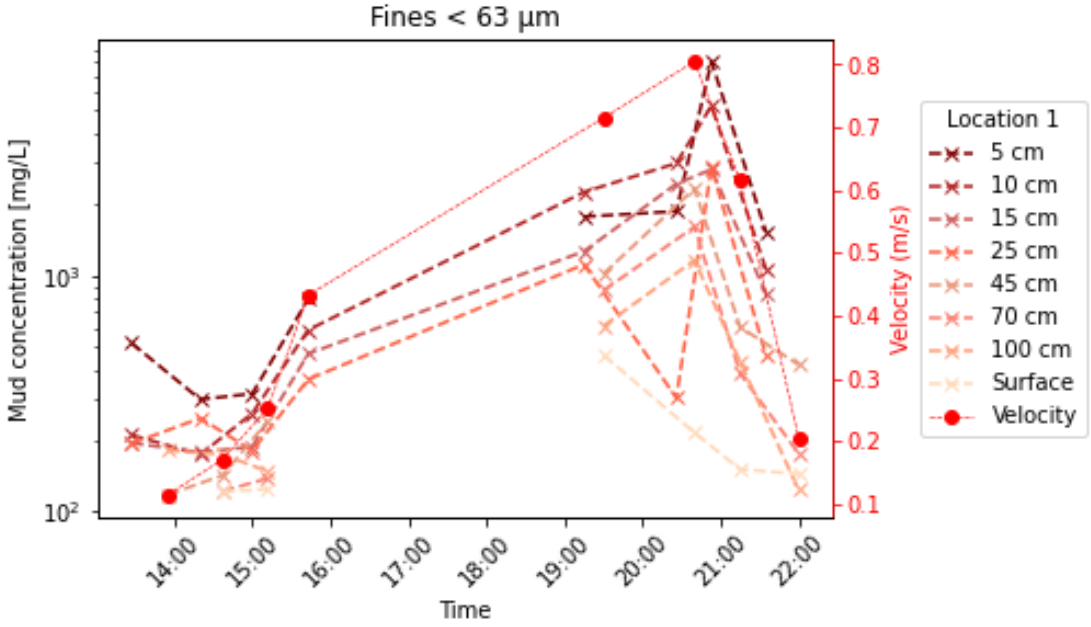

Figure A 5 Mud concentrations (fines< 63 µm) at various elevations above the bed and depth-averaged current velocity over tidal cycle; Day 1; 16 May 2022

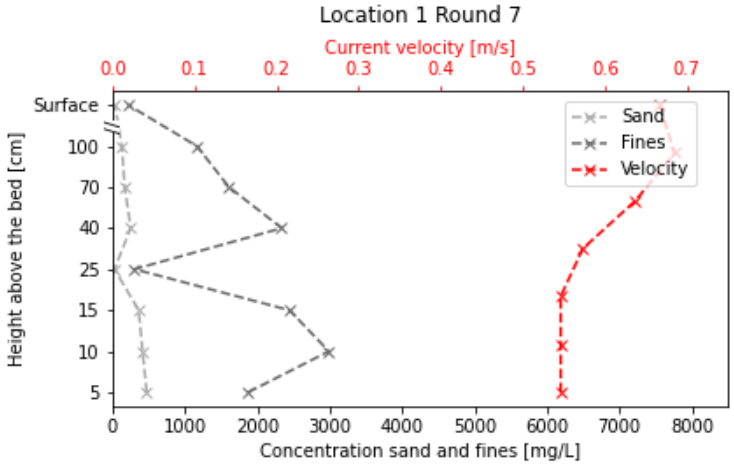

Figure A 6 Flow velocity, mud and sand concentration profiles in near-bed zone; Day 1, Time 20.26-20.40 (Round 7)

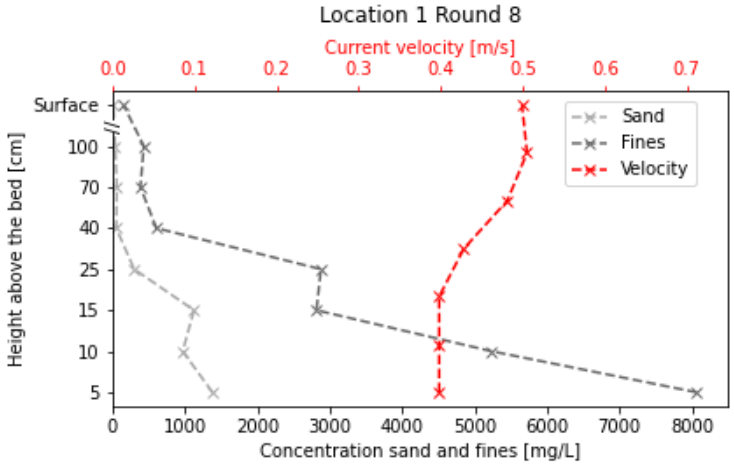

Figure A 7 Flow velocity, mud and sand concentration profiles in near-bed zone; Day 1, Time 20.53-21.15 (Round 8)

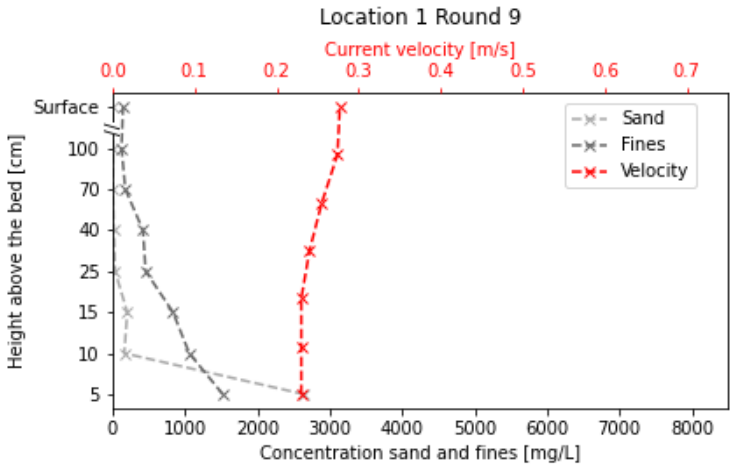

Figure A 8 Flow velocity, mud and sand concentration profiles in near-bed zone; Day 1, Time 21.35-22.00 (Round 9)

A.3 Data of Day 2-17 May 2022

The background data are given in Table A 5.

Table A 5 Background data; Day 2-17 May 2022

Location	2. Holwerd - Ameland Channel (53º24'13"N / 5º50'29"E)
Date	17 May 2022
Wind	4 bft
Water temperature	17.2 ºC
Wave height/period (estimated)	No waves
Bed level to Datum (NAP)	3.0 m
Type of bed sediment, d50 sand fraction	119.2
Type of suspended sediment	
Wet/Dry density of bed sample	1795;995
Percentage sand of bed sample	90%
Percentage of shells	No shells, <1%
Percentage of organic materials	Very little , <3%
Bed form data	Not measured
Sinking of bed fish in bed	Minimal < 5-10 cm – sandy site and the frame was rather stable

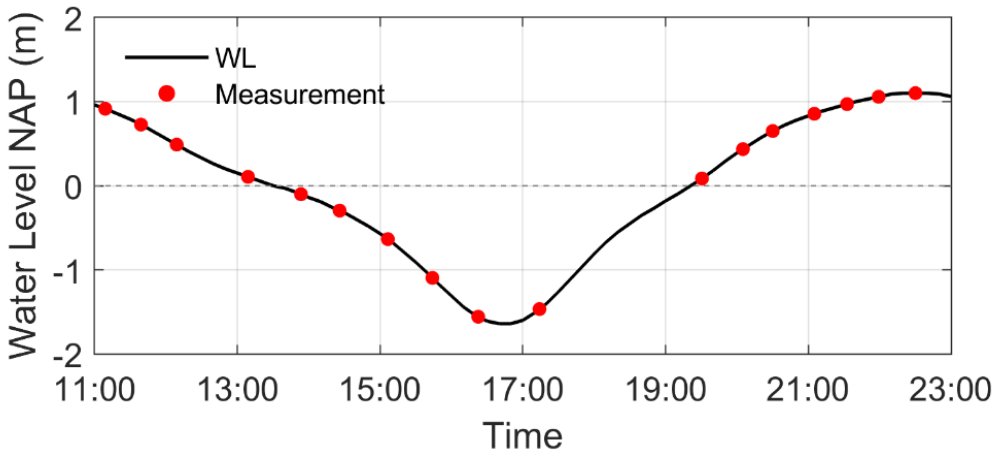

Figure A 9 Tidal water levels and sampling times on Day 2; 17 May 2022

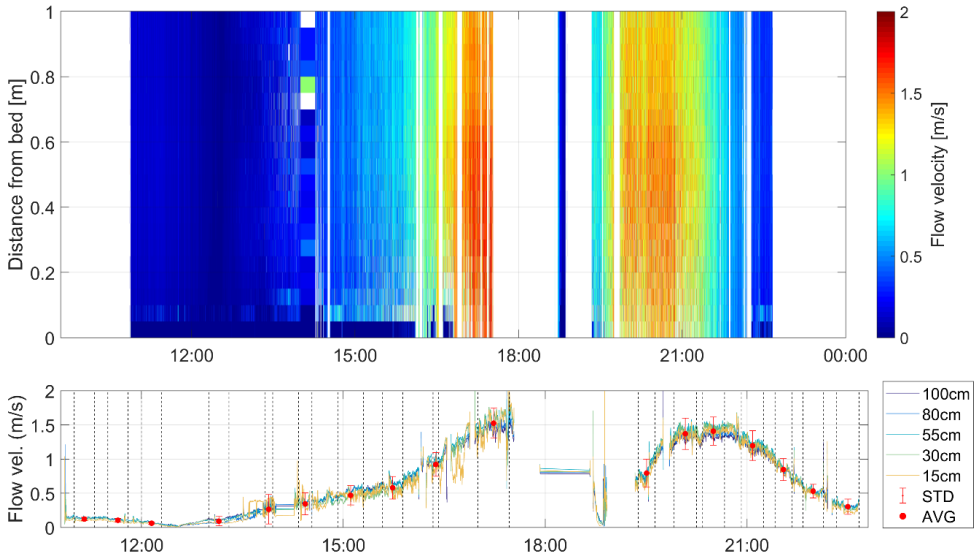

Figure A 10 Tidal current velocities on Day 2; 17 May 2022

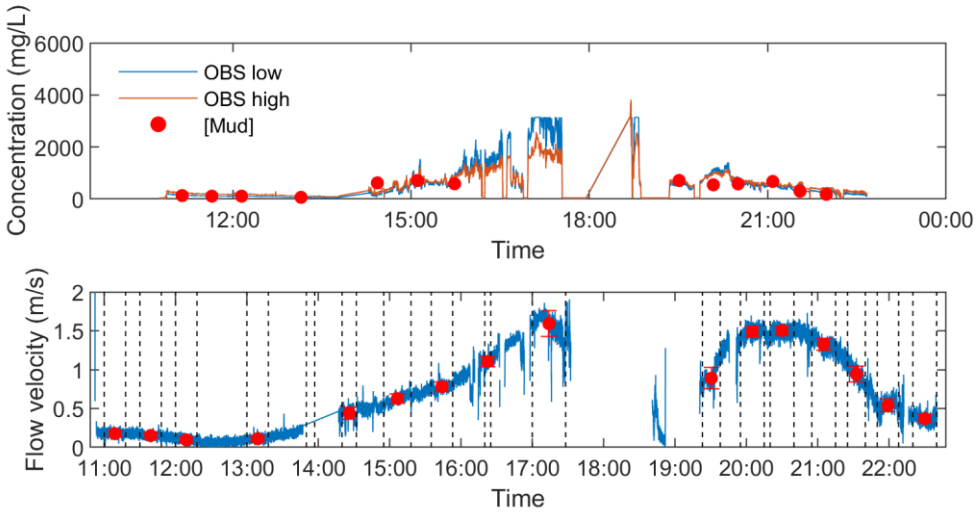

Figure A 11 Depth-averaged current velocities and mud concentrations on Day 2; 17 May 2022. Top Panel: Concentrations from samples [Mud] and OBS at 1 m above bed (low/high range instrument setting); red dot= average value of OBS-data; Bottom Panel: Aquadopp flow velocity at 1.2 m above bed; red dot=average value of flow velocity within a sampling cycle.

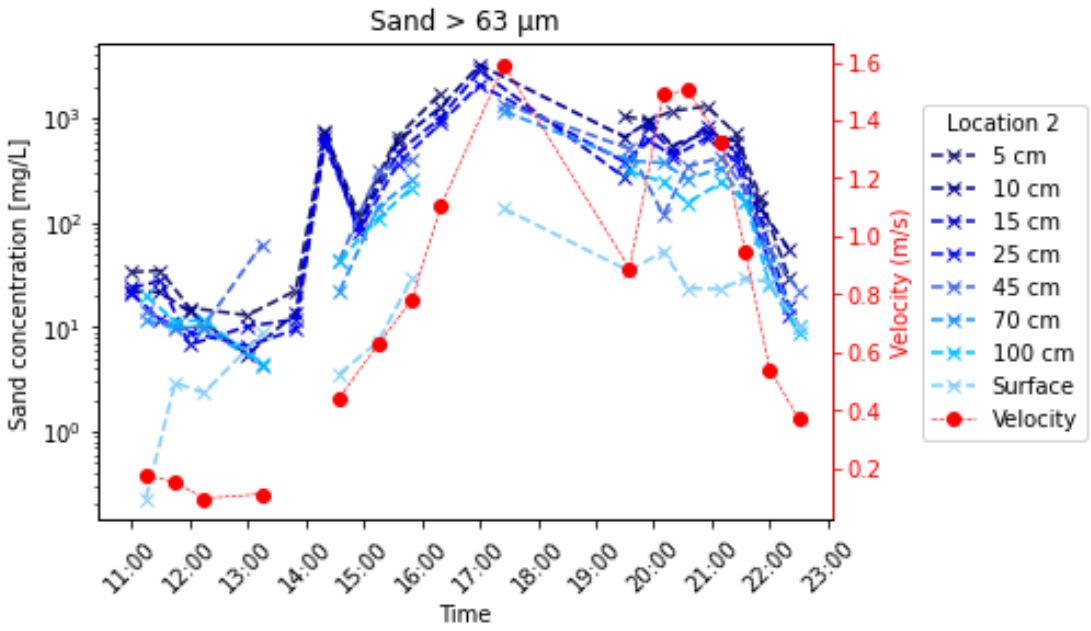

Figure A 12 Sand concentrations at various elevations above the bed and depth-averaged current velocity over tidal cycle; Day 2; 17 May 2022

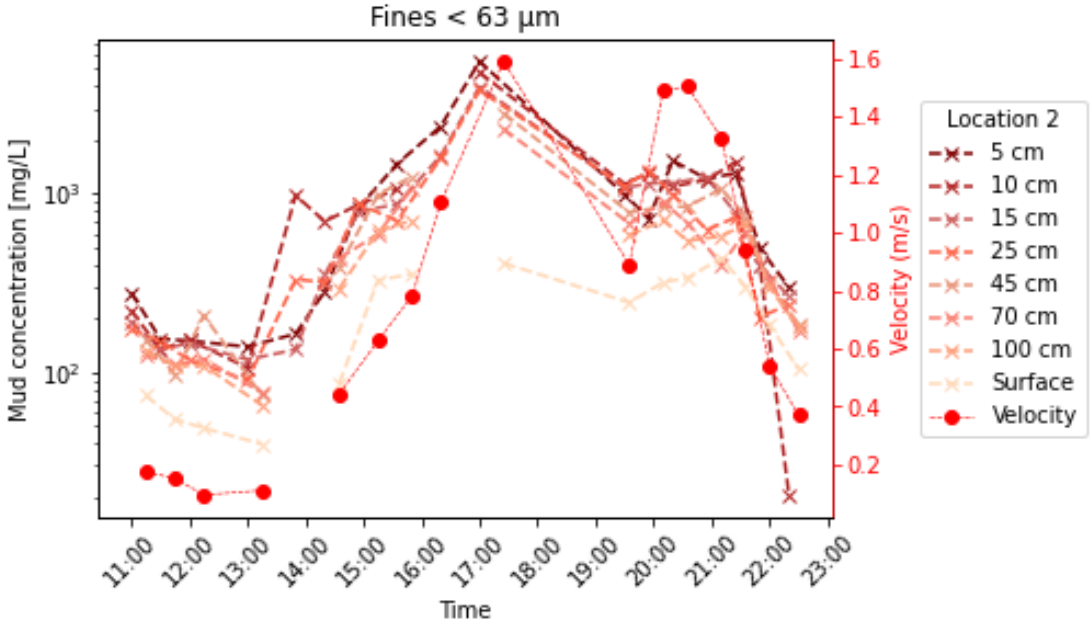

Figure A 13 Mud concentrations (fines< 63 µm) at various elevations above the bed and depth-averaged current velocity over tidal cycle; Day 2; 17 May 2022

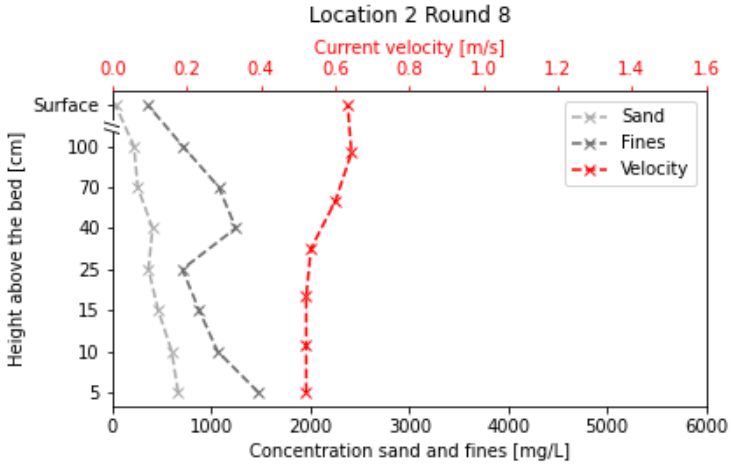

Figure A 14 Flow velocity, mud and sand concentration profiles in near-bed zone; Day 2, Time 15.35-15.50 (Round 8)

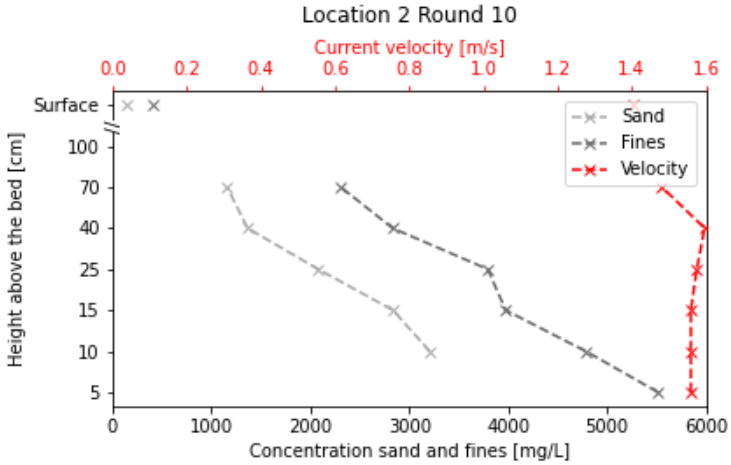

Figure A 15 Flow velocity, mud and sand concentration profiles in near-bed zone; Day 2, Time 17.00-17.25 (Round 10)

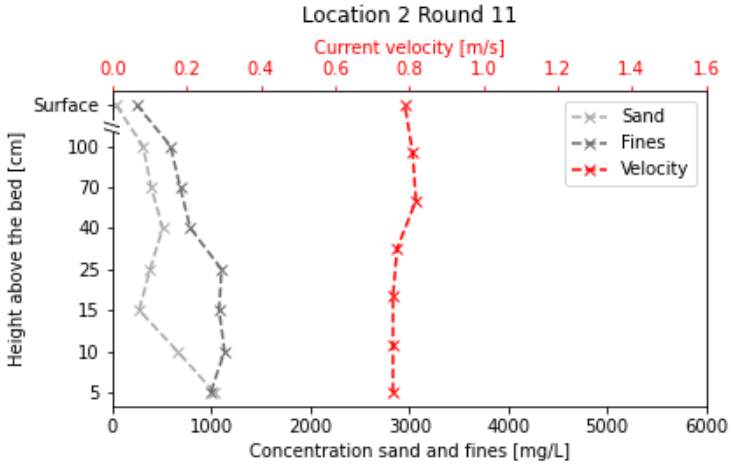

Figure A 16 Flow velocity, mud and sand concentration profiles in near-bed zone; Day 2, Time 19.30-1935 (Round 11)

A.4 Data of Day 3-14 June 2022

The background data are given in Table A 6.

Table A 6 Background data; Day 3; 14 June 2022

Location	3. Holwerd - Ameland Channel (53º23,563'N/ 5º51,958'E)
Date	14 June 2022
Wind	3 bft
Water temperature	17.9 ºC
Wave height/period (estimated)	No waves
Bed level to Datum (NAP)	2.25 m
Type of bed sediment, d_{50} sand fraction	82
Type of suspended sediment	fines and sand
Wet/Dry density of bed sample	1504;888
Percentage sand of bed sample	46%
Percentage of shells	No shells, <1%
Percentage of organic materials	Very Little OM, <3%
Bed form data	Not measured
Sinking of bed fish in bed	Possible sinkage up to 15 cm based on the ADCP signal. Although the frame was quite stable in this site.

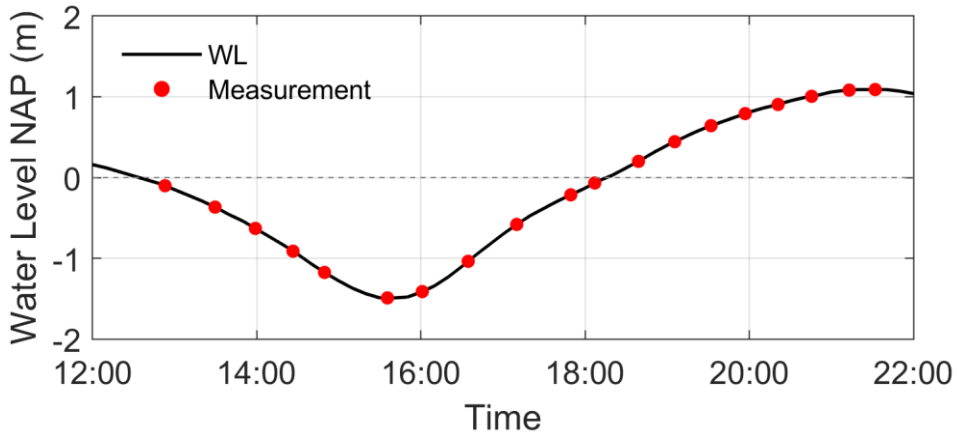

Figure A 17 Tidal water levels and sampling times on Day 3; 14 June 2022

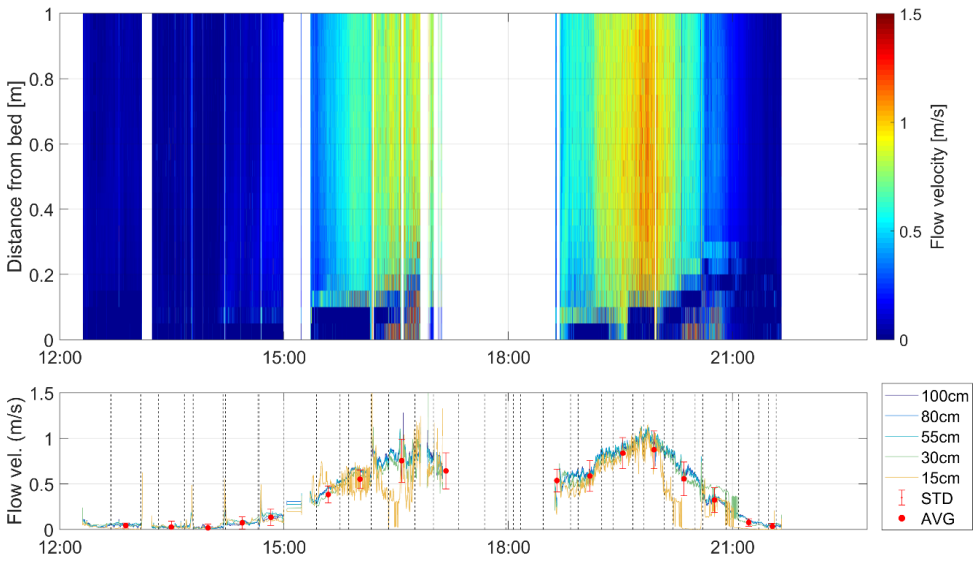

Figure A 18 Tidal current velocities on Day 3; 14 June 2022

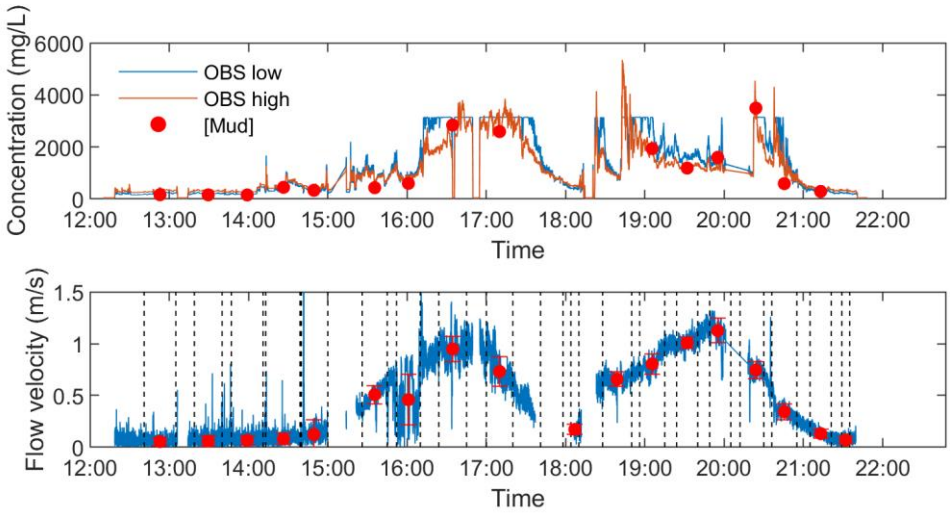

Figure A 19 Depth-averaged current velocities and mud concentrations on Day 3; 14 June 2022. Top Panel: Concentrations from samples [Mud] and OBS at 0.7 m above bed (low/high range instrument setting); red dot= average value of OBS-data; Bottom Panel: Aquadopp flow velocity at 1.2 m above bed; red dot=average value of flow velocity within a sampling cycle.

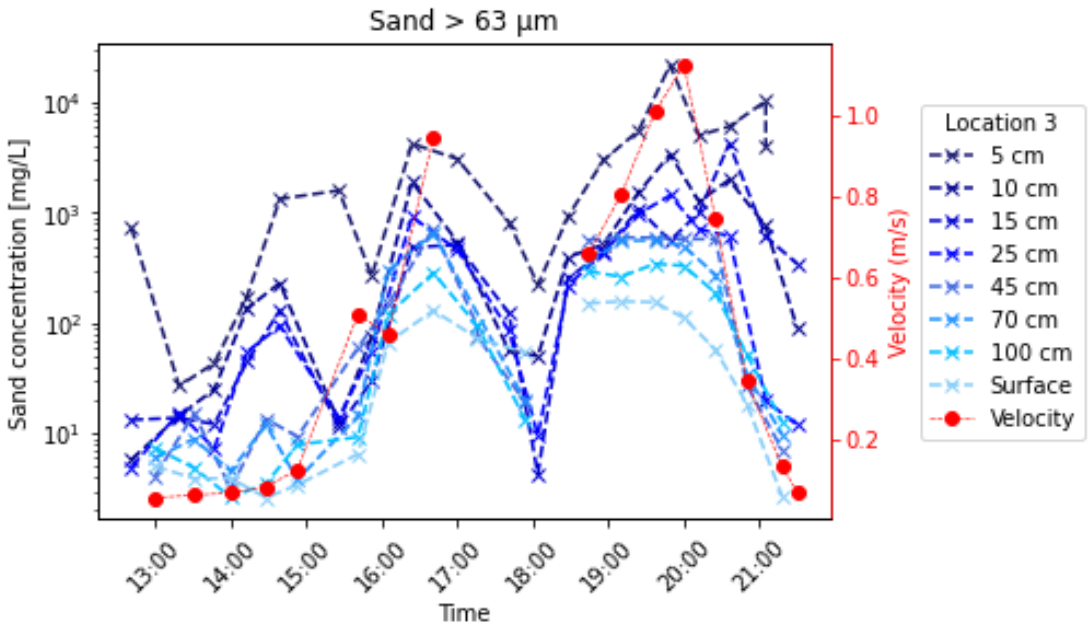

Figure A 20 Sand concentrations at various elevations above the bed and depth-averaged current velocity over tidal cycle; Day 3; 14 June 2022

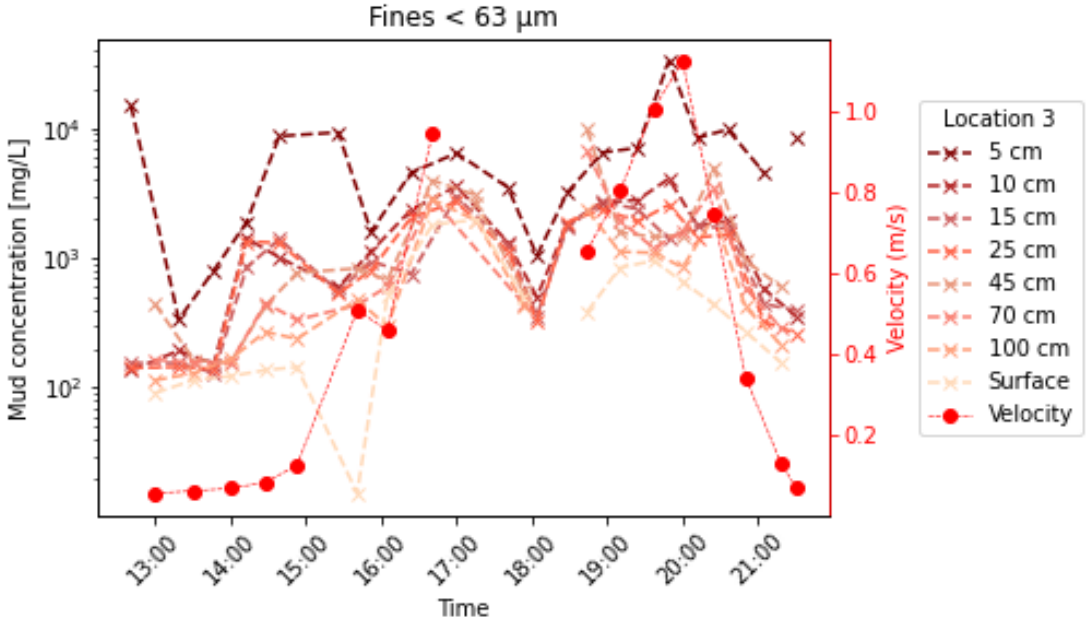

Figure A 21 Mud concentrations (fines< 63 µm) at various elevations above the bed and depth-averaged current velocity over tidal cycle; Day 3; 14 June 2022

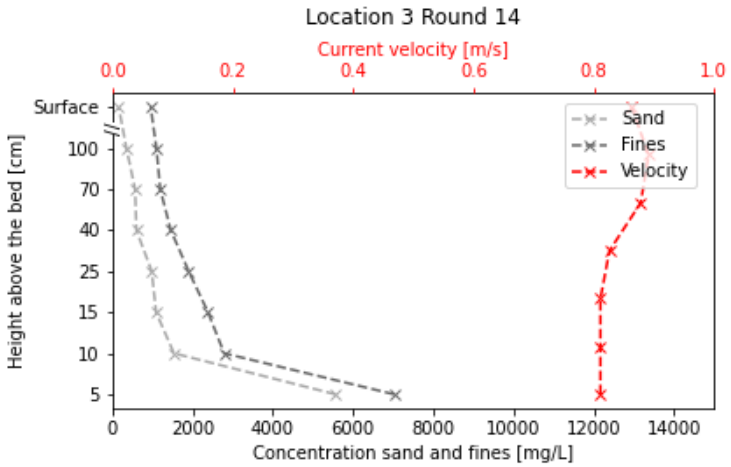

Figure A 22 Flow velocity, mud and sand concentration profiles in near-bed zone; Day 3, Time 19.24-19.37 (Round 14)

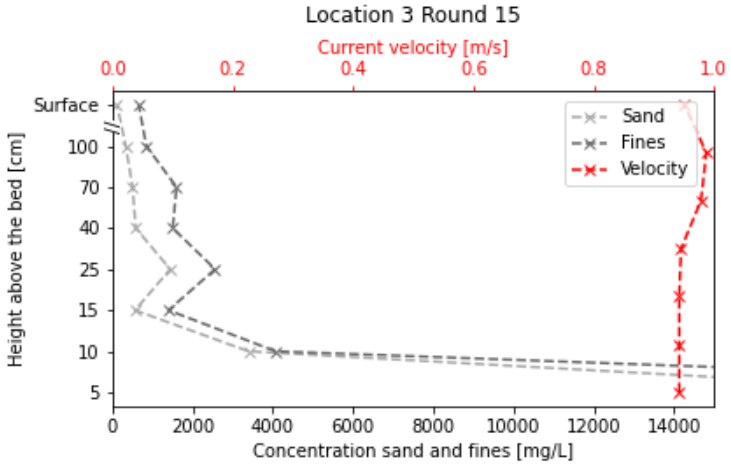

Figure A 23 Flow velocity, mud and sand concentration profiles in near-bed zone; Day 3, Time 19.49-20.00 (Round 15)

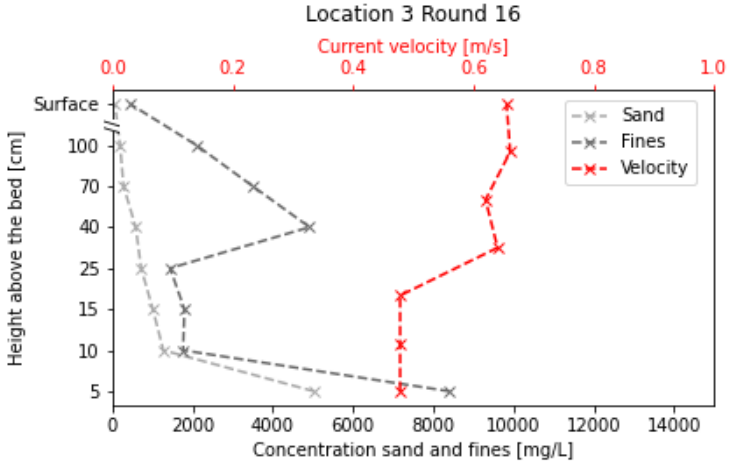

Figure A 24 Flow velocity, mud and sand concentration profiles in near-bed zone; Day 3, Time 20.12-20.25 (Round 16)

A.5 Data of Day 4-15 June 2022

The background data are given in Table A 7.

Table A 7 Background data; Day 3-14 June 2022

Location	4. Holwerd - Ameland Channel (53º23,544'N/ 5º51,128'E)
Date	15 June 2022
Wind	3 bft
Water temperature	18.8 ºC
Wave height/period (estimated)	No waves
Bed level to Datum (NAP)	3.7 m
Type of bed sediment, d_{50} sand fraction	122 μm
Type of suspended sediment	fines and sand
Wet/Dry density of bed sample	1521;709
Percentage sand of bed sample	66%
Percentage of shells	Some shells in the sample, ca. 10 %
Percentage of organic materials	Little OM, 3 %
Bed form data	Not measured
Sinking of bed fish in bed	Possible sinkage up to 10 cm based on the ADCP data. Frame was quite stable in this site as well.

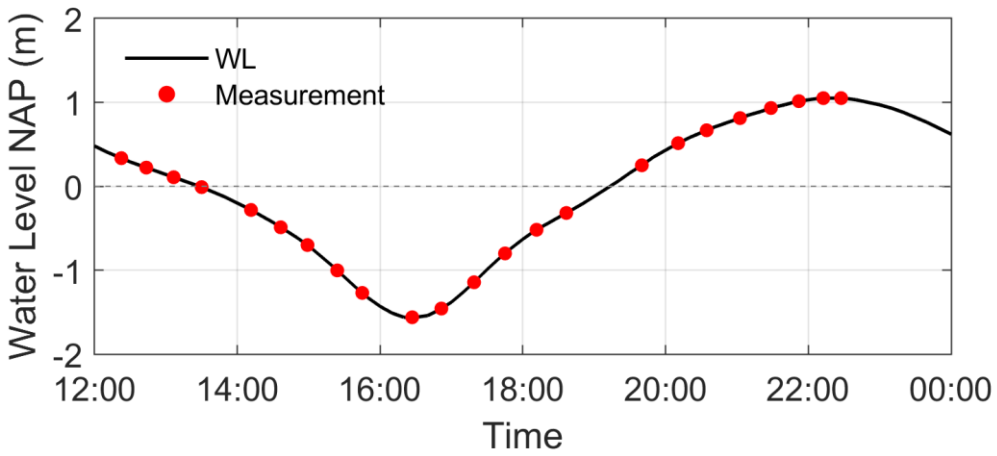

Figure A 25 Tidal water levels and sampling times on Day 4; 15 June 2022

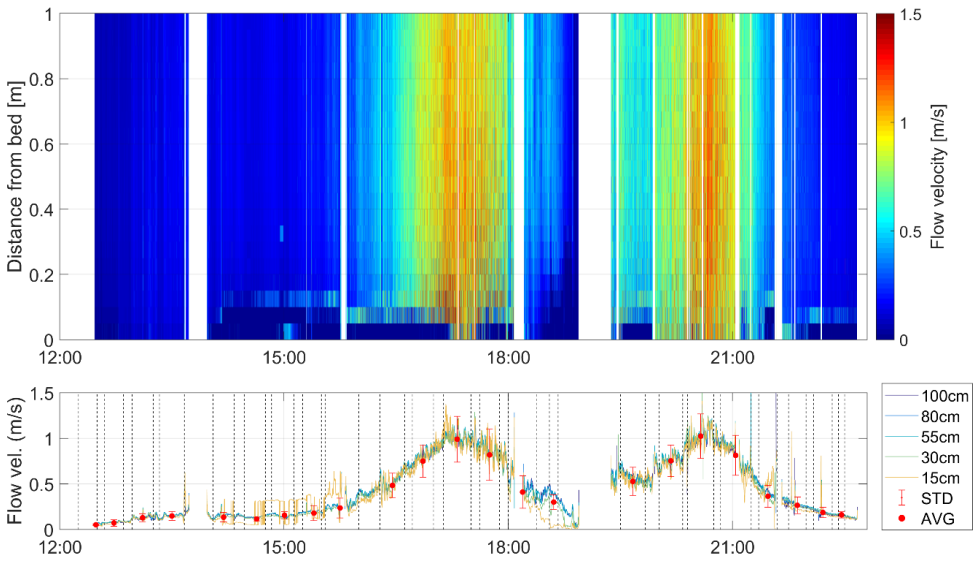

Figure A 26 Tidal current velocities on Day 4; 15 June 2022

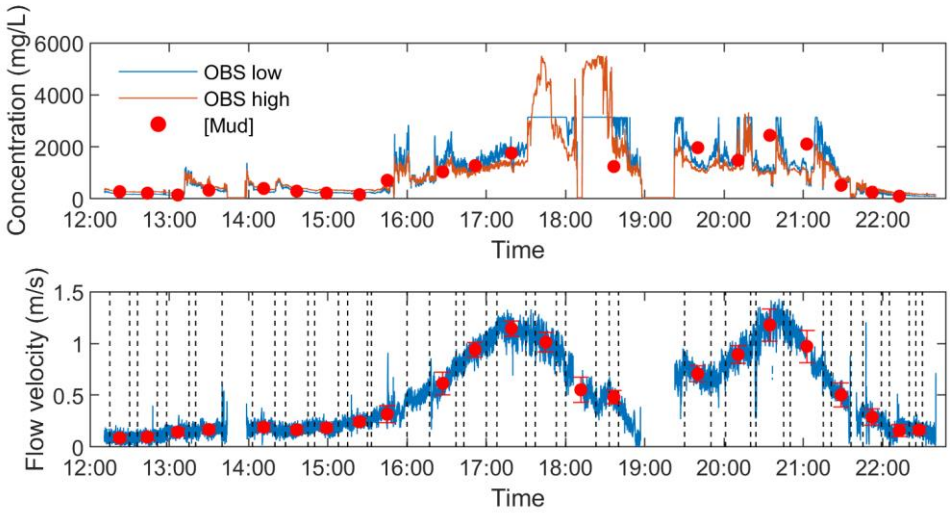

Figure A 27 Depth-averaged current velocities and mud concentrations on Day 4; 15 June 2022. Top Panel: Concentrations from samples [Mud] and OBS at 0.7 m above bed (low/high range instrument setting); red dot= average value of OBS-data; Bottom Panel: Aquadopp flow velocity at 1.2 m above bed; red dot=average value of flow velocity within a sampling cycle.

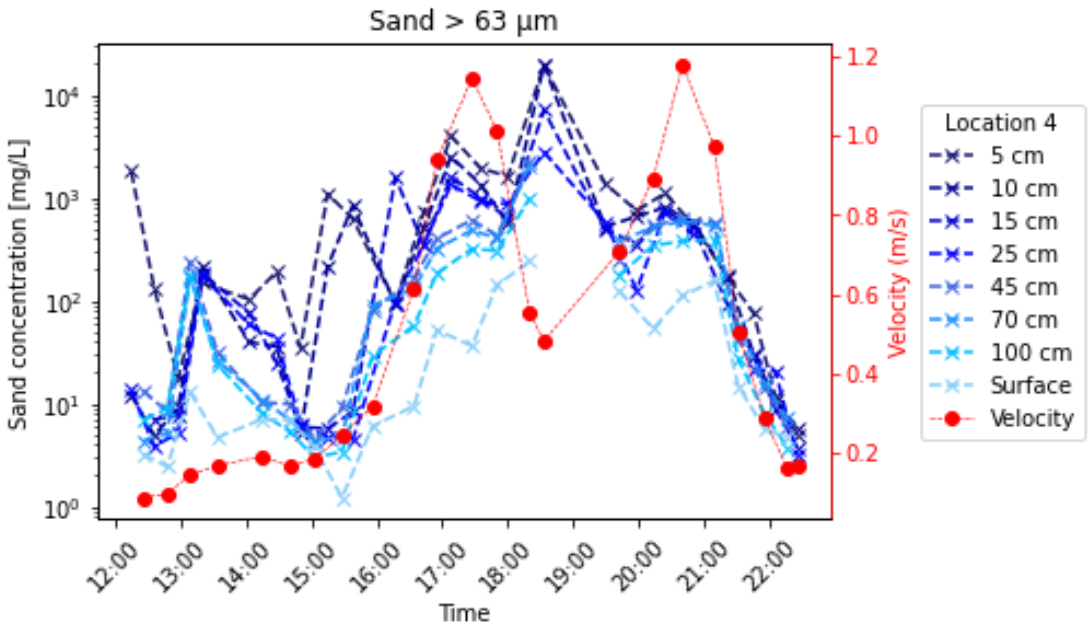

Figure A 28 Sand concentrations at various elevations above the bed and depth-averaged current velocity over tidal cycle; Day 4; 15 June 2022

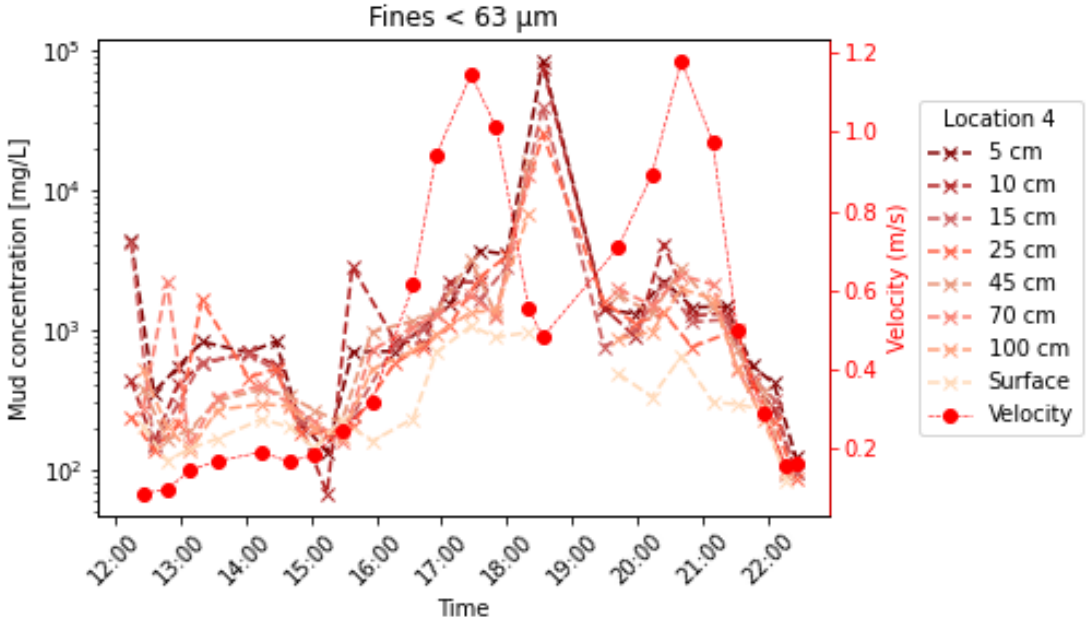

Figure A 29 Mud concentrations (fines< 63 µm) at various elevations above the bed and depth-averaged current velocity over tidal cycle; Day 4; 15 June 2022

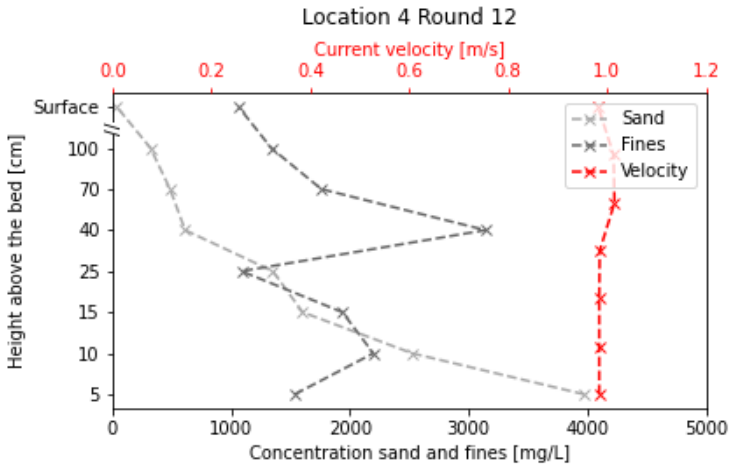

Figure A 30 Flow velocity, mud and sand concentration profiles in near-bed zone; Day 4, Time 17.08-17.27 (Round 12)

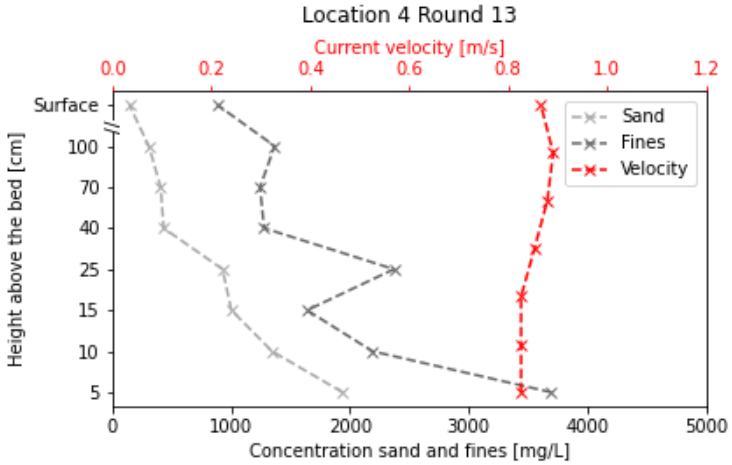

Figure A 31 Flow velocity, mud and sand concentration profiles in near-bed zone; Day 4, Time 17.35-17.50 (Round 13)

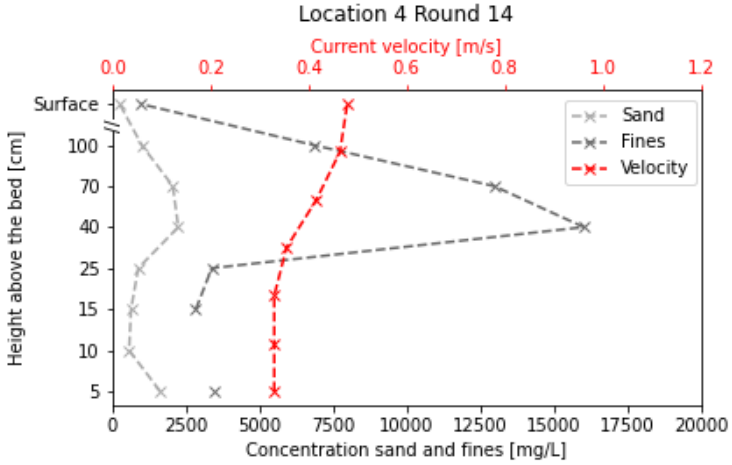

Figure A 32 Flow velocity, mud and sand concentration profiles in near-bed zone; Day 4, Time 18.00-18.20 (Round 14)

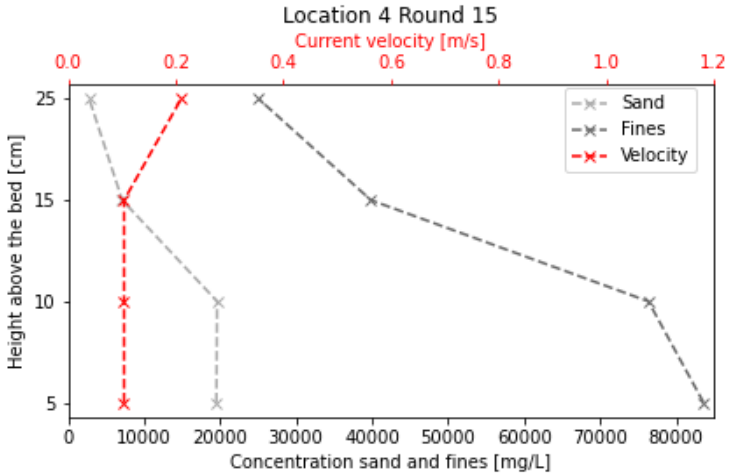

Figure A 33 Flow velocity, mud and sand concentration profiles in near-bed zone; Day 4, Time 18.33-19.00 (Round 15)

A.6 Calibration of OBS-sensor

The OBS (Optical Backscatter) was calibrated for SSC (mg/L) based on the in-situ samples.

The calibration was defined following the curve fit for both low range and high range sensors (Figure A 35 and Figure A 36). The low range captures the lower concentrations with higher resolution while the high range offers measurements with lower resolution up to higher sediment concentrations. Spurious values beyond the sensor measurement range were removed.

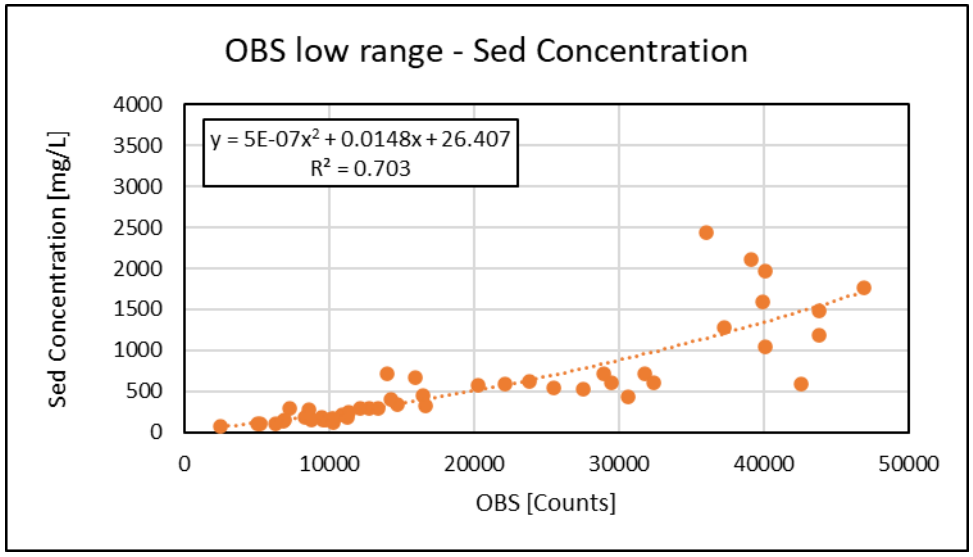

Figure A 34 Calibration of the low range OBS sensor against measured sediment concentrations.

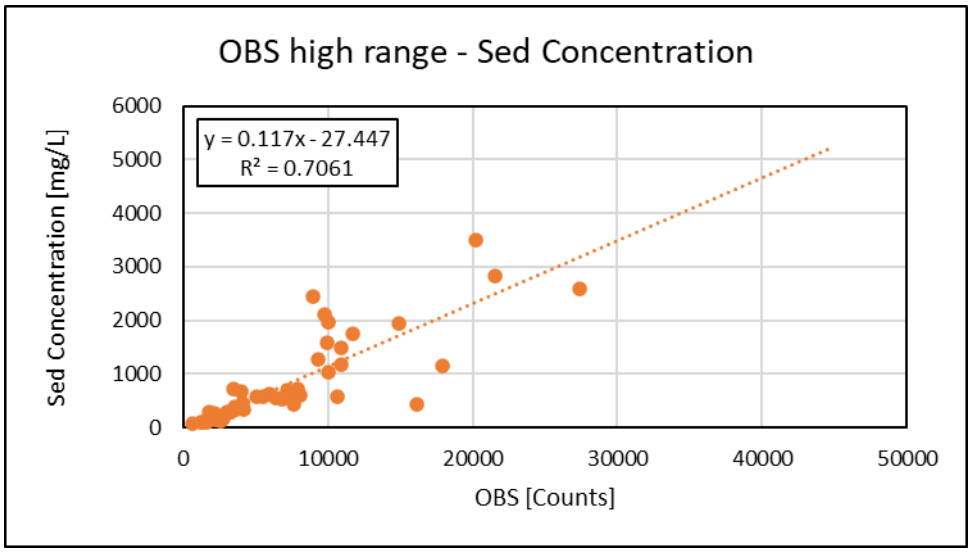

Figure A 35 Calibration of the high range OBS sensor against measured sediment concentrations.

The low range OBS calibration was obtained with RMSE of 316mg/L and the high range 435mg/L.

B Summary of field measurements from Holwerd, 2019

Detailed measurements of mud and sand transport at 4 locations in the tidal ferry channel Holwerd-Ameland have been done by WaterProof in the period of February-March 2019 and September-October 2019. The following data have been collected (see also Table B.1):

- continuous measurements of current velocity , water levels, wave heights and mud concentrations (OBS-sensors) using 2 bed frames;
- discharge measurements over 13 hours in 10 cross-sections;
- sediment transport measurements over 13 hours consisting of: velocity, mud/sand concentrations at various points in the water column by pump samples;
- bed samples at 13 locations;
- water-sediment samples (suspension samples) at various points of the water column (lowest sampling point at 0.2 m above the bed) for determination of settling velocities by settling tests.

The most important transport phenomena occurring in the ferry channel are summarized, as follows:

- peak flood velocities are in the range of 0.6 to 0.9 m/s occurring at about 4 to 5 hours before High Water; the peak flood velocity values are somewhat higher at locations 1 and 2 most close to the landing pier at Holwerd; peak ebb velocities generally are somewhat lower than the peak flood velocities;
- depth-averaged mud concentrations generally are maximum in the period of maximum flood/ebb flow or shortly after that (within 1 hour); peak values are in the range of 500 to 5000 mg/l at locations 1 and 2 and somewhat lower at locations 3 and 4 further away from the landing pier;
- mud concentrations decrease rapidly in periods with decreasing flow velocities due to relatively high settling velocities in the range of 1 to 3 mm/s (coarse silt);
- mud concentrations are relatively low (range of 100 to 200 mg/l; fine silt) around slack tide with low velocities;
- depth-averaged mud concentrations are high during storm conditions (BF7/8); 2000 to 10000 mg/l during a periods of 2 hours around maximum flow ebb/flood; lower values of 500 to 1000 mg/l around slack tide with low velocities;
- depth-integrated mud transport in the period of maximum flow is mostly in the range of 0.5 to 5 kg/m/s;
- sand concentrations and depth-integrated sand transport are much lower than the mud concentrations and transport values (factor 5 to 10).

Table B.1 Summary of field data 2019 in ferry channel near Holwerd (NL).

Season	Date	Location (km to ferry landing point)	Bed to NAP (about MSL)	Wind (BF-scale)	Tide (Neap=1.6 m; Spring=3 m; Mean=2.3 m)	
					Astronomical	Measured
Winter	7 Feb.i 2019	2 (1,7 km)	-2 (±0,3)	7 sw	2.2	2.4
	8 Feb.i 2019	1 (-0,3 km)	-2.2 (±0,3)	7/8 s	2.3	2.4
	20 Feb. 2019	4 (6,5 km)	-6.5 (±1,0)	4 sw	2.8	2.5
	21 Feb. 2019	3 (3,7 km)	-3.7 (±0,4)	4 sw	2.8	2.5
	26 Feb. 2019	1 (-0,3 km)	-2.4 (±0,3)	2 s	2.8	2.4
Summer	25 Sep. 2019	1 (-0,3 km)	-2.4 (±0,3)	4 s	1.9	2.0
	26 Sep. 2019	4 (6,5 km)	-5.5 (±1,0)	5 s	2.2	2.4
	27 Sep. 2019	3 (3,2 km)	-3.5 (±0,3)	6 s	2.5	2.4
	1 Oct. 2019	2 (1,7 km)	-2.3 (±0,3)	4 s	2.8	3.0

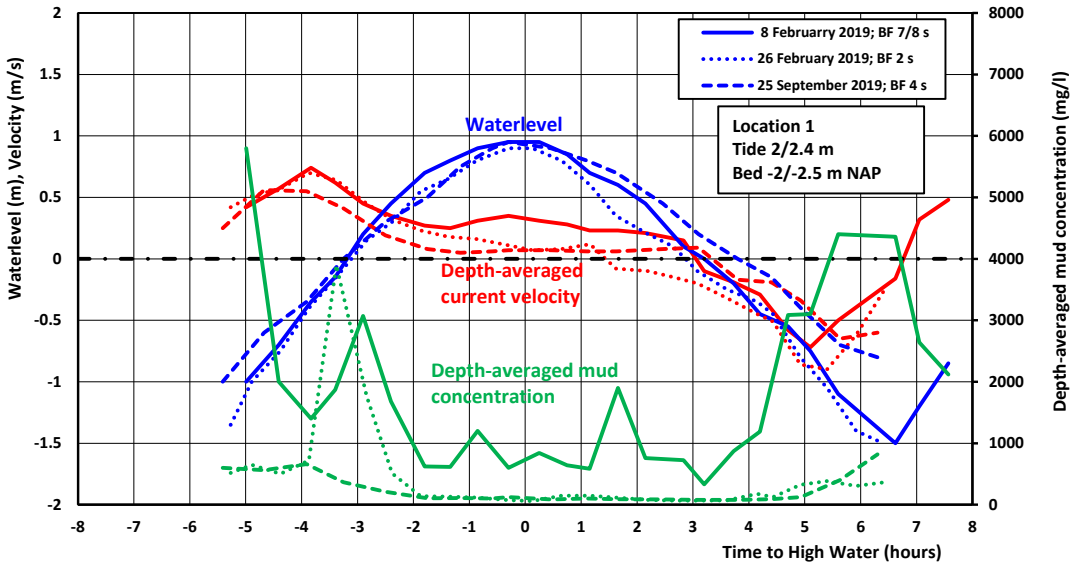

Figure B1 Current velocities and mud concentrations over tidal cycle, location 1; ferry channel Holwerd

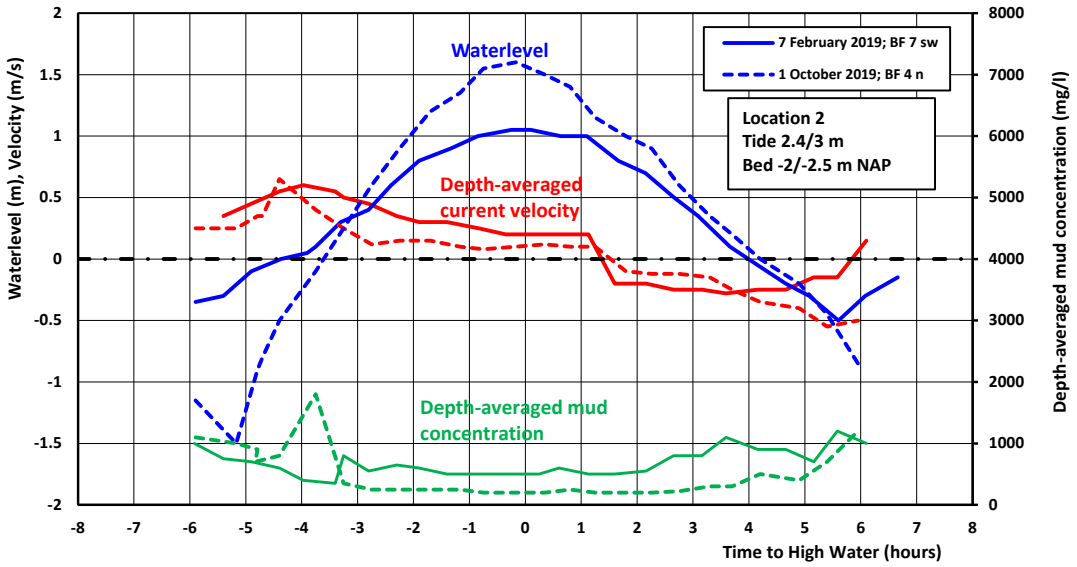

Figure B2 Current velocities and mud concentrations over tidal cycle, location 2; ferry channel Holwerd

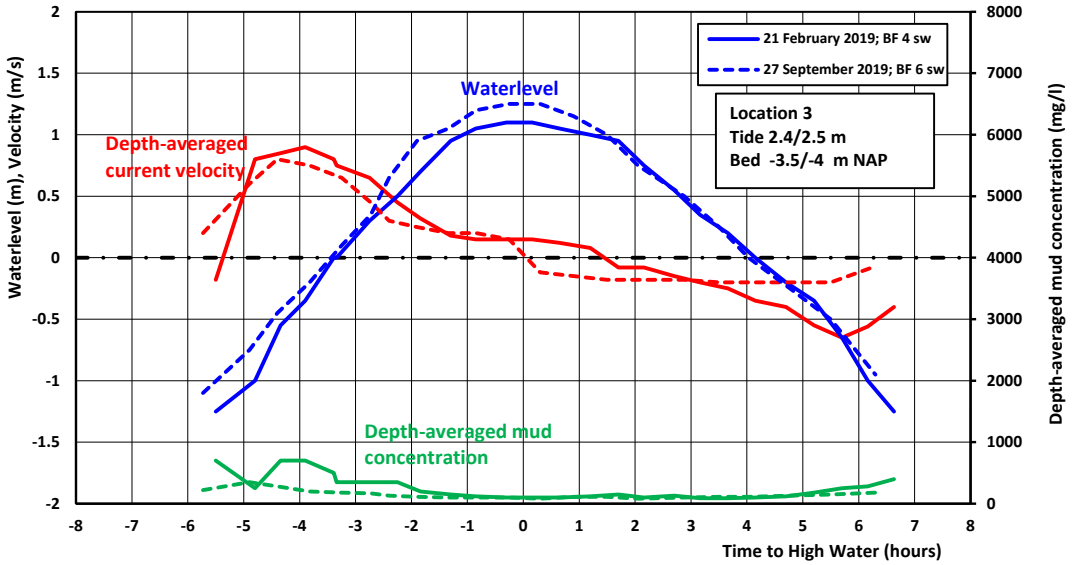

Figure B3 Current velocities and mud concentrations over tidal cycle, location 3; ferry channel Holwerd

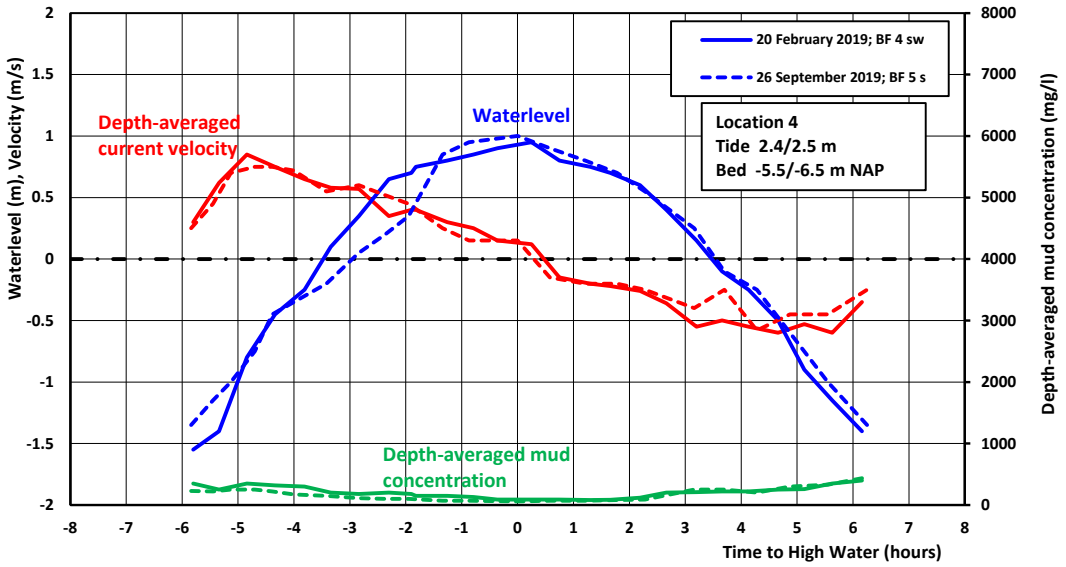

Figure B4 Current velocities and mud concentrations over tidal cycle, location 4; ferry channel Holwerd

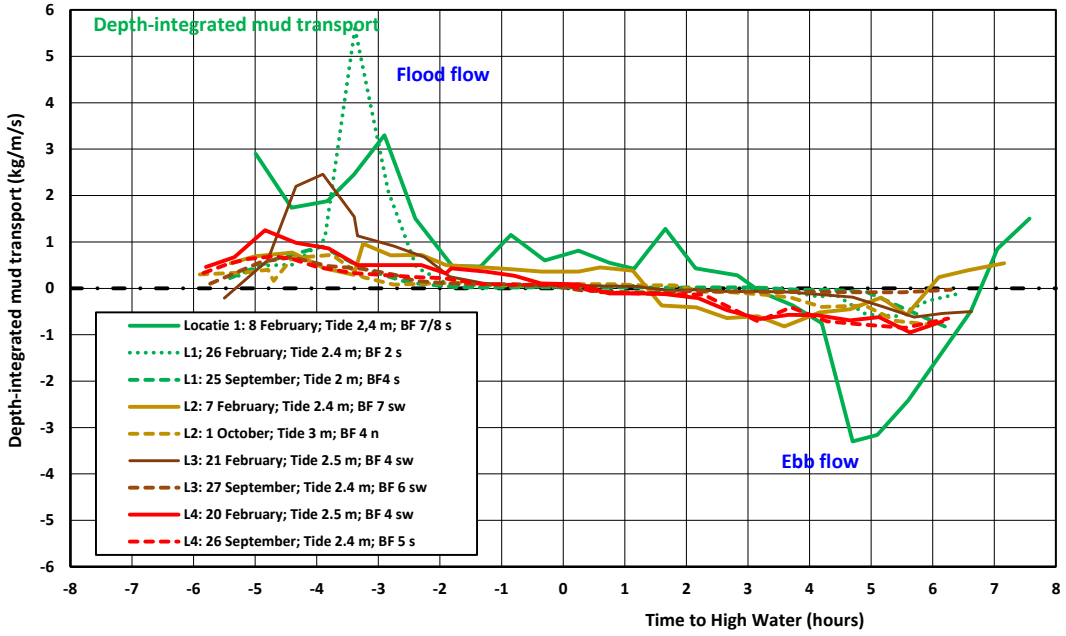

Figure B5 Depth-integrated mud transport over tidal cycle, location 1,2,3,4; ferry channel Holwerd

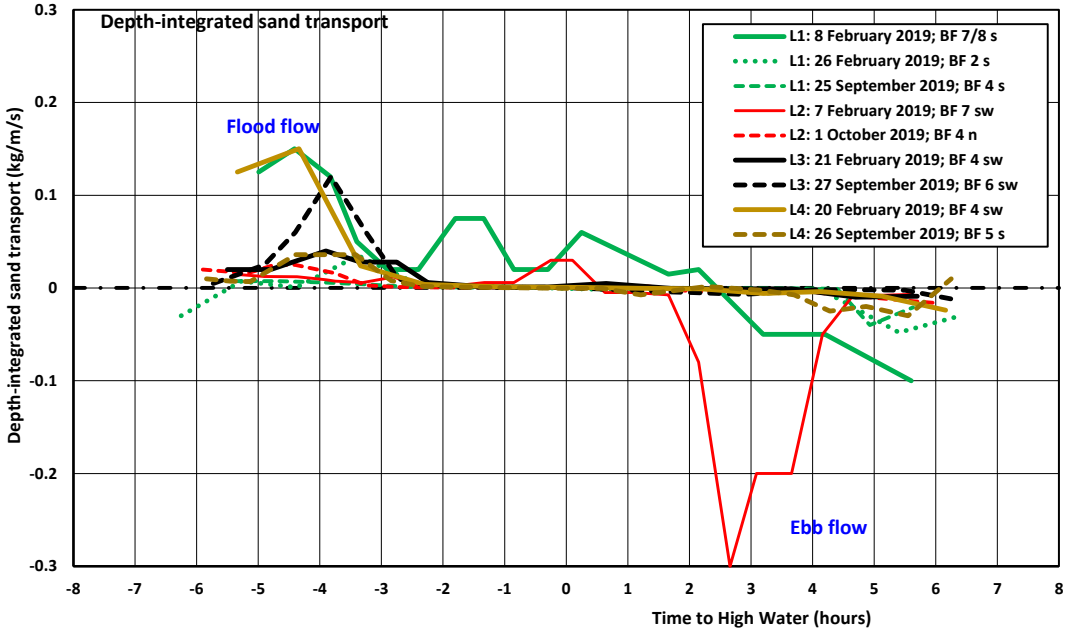

Figure B6 Depth-integrated sand transport over tidal cycle, location 1,2,3,4; ferry channel Holwerd